THE MESSENGER

EL MENSAJERO

ESO

La Silla
La Serena
Santiago
Munich

23.12.86

No. 45 – September 1986

New Interstellar Molecule Detected

P. CRANE, ESO

The molecule ^{13}CN has been detected for the first time in the interstellar medium. This isotopic analogue of the better known ^{12}CN molecule was discovered serendipitously in data which had been taken in order to measure the Cosmic Background Radiation temperature using the CN molecule. The European Southern Observatory's 1.4 metre Coudé Feed Telescope and associated Coudé Echelle Spectrograph with the Reticon detector was used for this work. In order to detect very weak features in the spectrum of the star ζ Ophiuchi, high resolution and high signal to noise spectra were obtained. It was subsequently realized that the ^{13}CN line should be visible in these data. A further analysis to search for this line was successful.

Figure 1 shows a plot of a portion of the observed spectrum and indicates the newly discovered line. This new line is the R(0) line of the 0,0 band of the $B^2\Sigma - X^2\Sigma$ electronic system of ^{13}CN, and its equivalent width is 0.179 ± 0.040 mÅ. For comparison the line of the more abundant ^{12}CN molecule has an equivalent width of 7.646 ± 0.091 mÅ.

In order to detect this line with certainty, observations from seven nights were combined to provide the final results. The line was present at about the 2 sigma significance level in the data from each night but the true significance of the detection was only evident after combining the data from several nights. The total integration time on the star was in excess of 25 hours.

The newly detected feature of ^{13}CN allows a determination of the carbon isotope ratio in the interstellar cloud in the direction of ζ Oph. The ^{12}C/^{13}C ratio determined from these measurements is 50 (+13; −10). This can be compared to

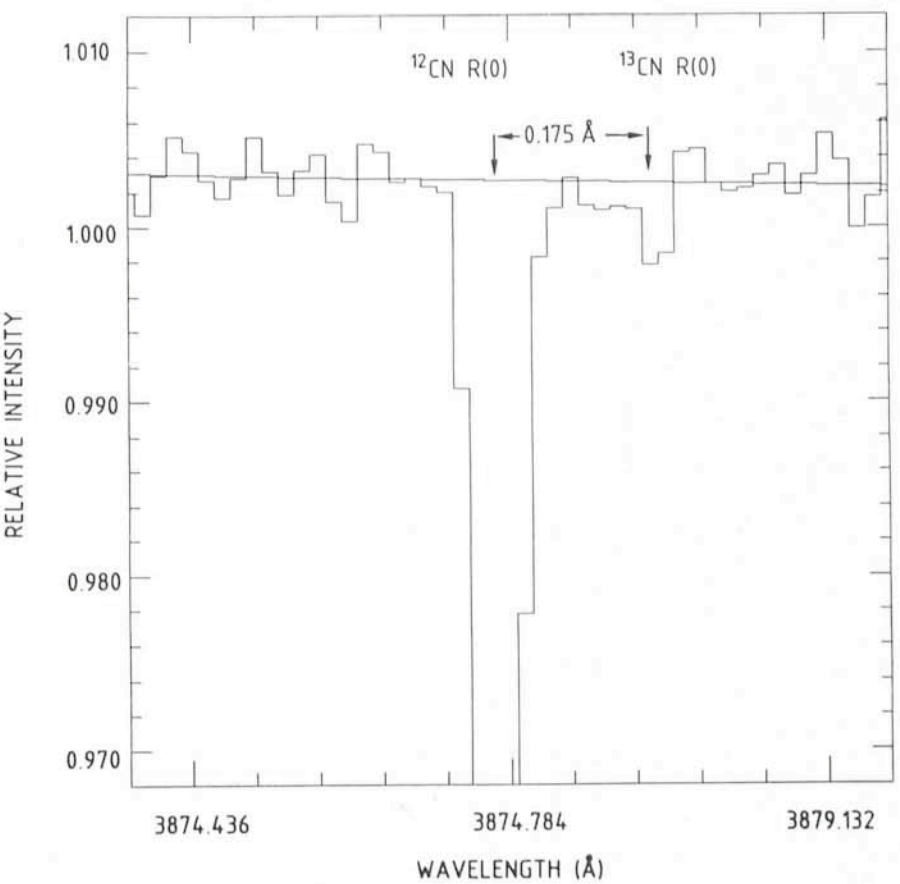

Figure 1: *Plot of the spectrum of the CN R(0) lines near 3875 Å. The upper panel shows range of intensities. The lower panel shows an expanded vertical scale and indicates the weak ^{13}CN feature.*

the terrestrial ratio of 89 and further substantiates theories of the enrichment of ^{13}C in the interstellar medium through evolution of the galaxy since the formation of the solar system. This value also agrees with other recent determinations of the $^{12}C/^{13}C$ ratio from the molecules $^{12}CH^+/^{13}CH^+$ and $^{12}CO/^{13}CO$. Since it had been speculated that ^{13}C might preferentially form CO compared to ^{12}C, the agreement between the CO, CN, and CH^+ abundances indicates that this effect is not very important.

The detection and measurement of weak features requiring high precision and high spectral resolution such as those reported here are a typical example of the way in which the new generation of very large telescopes which should become available early in the next decade can be exploited.

The Work of the ESO Observing Programmes Committee

M.C.E. HUBER, Institut für Astronomie, ETH Zürich, Chairman of the OPC
J. BREYSACHER, ESO

ESO astronomers devote considerable time to preparing, and put obvious care into writing Applications for Observing Time at La Silla. Many take justifiable pride in the presentation of their ideas. Yet, given the heavy oversubscription of telescope time, inevitably a selection of the proposed observing programmes must be made. And often this selection is drastic: in each Observing Period, the applied-for number of observing nights for the various telescopes exceeds the number of available nights by factors of two, at telescopes of intermediate size, to four, at the 2.2-m and 3.6-m telescopes!

It is the task of the Observing Programmes Committee (OPC) to evaluate the scientific merit of the submitted Applications. Based on the OPC's recommendations, ESO then prepares an Observing Schedule – employing the available telescope nights for the best-rated proposals. In the following we will describe the refereeing system of the OPC and explain the steps that lead to the final Observing Schedule on the ESO telescopes.

The history and procedures of the OPC have already been described by the previous OPC chairman, B. Westerlund, in 1982 (Messenger No. 28). In the meantime, the working procedures of the Committee have evolved considerably, so that an updated description is warranted.

The OPC in its current form exists since 1971: there is one Member and one Substitute member from each of the eight ESO countries*, they are designated by the National ESO Committees and serve for five-year terms.

Refereeing the Applications

The eight OPC Members, together with one ESO staff member (usually the Head of the Scientific Group, J. Danziger) referee the 300 to 350 Applications for Observing Time that are currently submitted for every six-month Observing Period (cf. Fig. 1).

Each Application is evaluated by three referees. As a result, each OPC Member has to read and rate over 100 Applications twice a year: he must decide on a mark for each proposed programme and recommend the number of nights that – in his judgement – should be made available to the applicant(s), if the programme actually receives telescope time. The rating scale comprises nine grades (extending from "outstanding" to "useless") that are expressed by numbers 1 to 5 with half-integer steps.

Rating over one hundred individual Applications is not only a demanding, but also a very time-consuming undertaking. This is the reason why so much emphasis is put on concise Applications! OPC Members spend more than the equivalent of one working week in fulfilling this task. A new Member (or a Substitute Member replacing the regular Member) may find that up to two weeks full-time are needed to arrive at a consistent judgement of all the Applications he has to referee. Furthermore, the handling of Applications – from receipt by ESO until the moment when applicants are informed on whether observing time for their proposal(s) can be granted or not – follows a rather tight schedule, giving the OPC Members only about three weeks to evaluate the proposals.

In order to avoid any bias in judgement, some of the referees assigned to a given applicant (or group of appli-

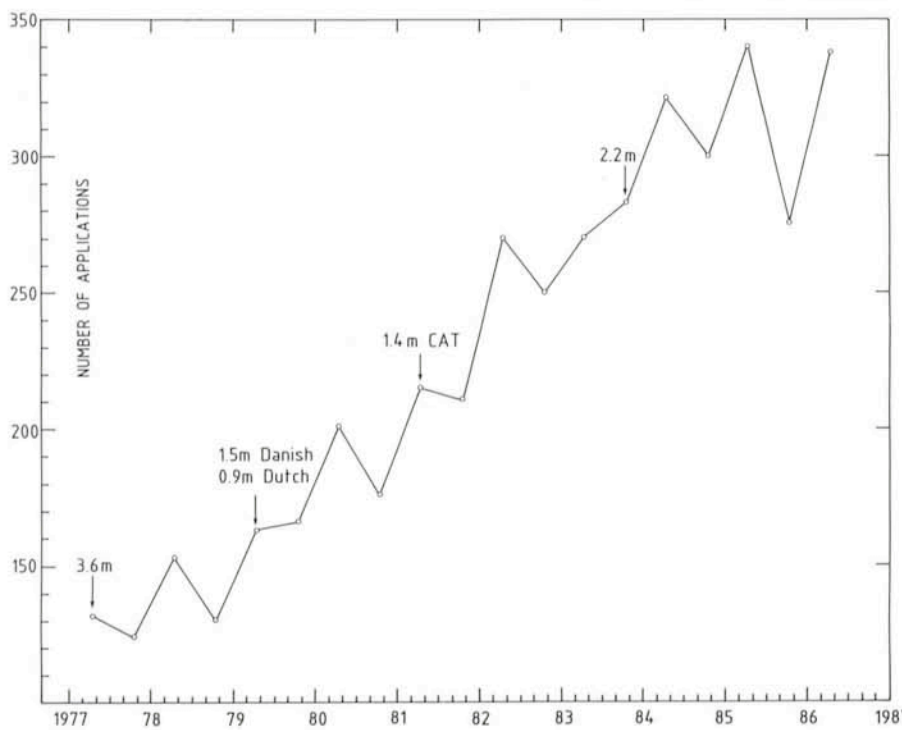

Figure 1: *Number of Applications submitted to ESO during the past nine years. Arrows indicate when new telescopes became available.*

* This year's composition of the OPC is (with Substitute Members in parentheses): J.-M. Vreux (and E.L. van Dessel), Belgium; E.H. Olsen (and P.E. Nissen), Denmark; G. Monnet (and J. Boulesteix), France; K. Fricke (and I. Appenzeller), Federal Republic of Germany; A. Renzini (and F. Bertola), Italy; P.C. van der Kruit (and K.A. van der Hucht), The Netherlands; G. Lynga (and L. Nordh), Sweden; and M.C.E. Huber (and B. Hauck), Switzerland. The OPC Members (and their terms) are listed regularly in the ESO Annual Report.

cants) are changed from one Observing Period to the next. Given the limited number of OPC Members, a particular Application is thus evaluated by specialist as well as non-specialist referees. Accordingly, applicants have to make their proposed observations appealing to specialists and non-specialists alike. They must both, demonstrate their competence within a specific area and show the importance of the proposed work in the broader context. Since any large discrepancy in the ratings will be discussed at the semi-annual OPC Meetings, faulty judgements on the side of the non-specialist (or specialist!) will be eliminated.

Preliminary Observing Schedule

When the ratings and recommended numbers of nights from the referees are available, ESO produces a list of the Observing Applications for each telescope, with the Applications being ranked according to the average ratings of the three referees. The average recommended number of nights is used to sum up the observing time required as one goes down the list, and a cutoff line is drawn, when the number of nights available for astronomy (technical time being considered separately) is reached. (Applications where doubt about the feasibility was expressed by at least one referee are listed apart.) The information contained in this list is also used to generate a set of tables which shows the distribution of the programmes above the cutoff line over the months and the moon phases for each telescope. This set of tables also shows the resulting change-overs of instruments for each telescope. These working documents, which actually represent preliminary observing schedules for the various telescopes, are sent to the members a few days before they get together in the OPC Meeting.

OPC Meetings

The OPC meets twice a year (i.e., once for each Observing Period) during two days. Most of the meeting time is spent in clarifying discrepancies in the judgement of Applications. The deliberations take place in the presence of the Director General and the Head of the Section Visiting Astronomers. The record of the meeting is kept by Mrs. Chr. Euler. Thus, a dozen people attend the OPC Meetings. The size of this group permits a frank and uninhibited discussion. It is important to note that this discussion is based on the scientific merit of the Applications alone: the national origin of an applicant is of no concern to the OPC.

Obviously, not all Applications can be discussed at a two-day meeting. Nevertheless, the preliminary schedule for each telescope is closely inspected.

First, those few Applications where doubt about feasibility had been expressed are scrutinized, one by one – and, if justified, are reinstated into the main list.

Next, Applications where the referees disagree in their ratings, are discussed in detail. The three OPC Members who had evaluated the Application in question are asked to explain why and how they arrived at their mark; and in the ensuing discussion, which usually involves the other OPC Members too, an effort is made to arrive at a more uniform judgement. In some cases, nevertheless, discrepant marks are left unaltered; this then reflects an honest difference of opinion between peers!

The influence of these discussions on the scientific judgement of the OPC Members (and, in the end, this *is* the scientific policy of the OPC!) cannot be overestimated. For these frank and spontaneous interchanges, the limited size and confidential nature of OPC Meetings is essential.

To further foster a "unité de doctrine" in the OPC, the Members may ask for discussion of any Application. In fact, referees will often earmark long-term observing programmes for a joint review of progress. Referees will also point out similar proposals with the same goal; the OPC will then seek to avoid unneeded duplication.

OPC Members are aware of the danger that they may (as committee members usually do) give preferential marks to "safe" Applications, which promise minor, but almost guaranteed progress. Such an attitude would be to the detriment of bolder Applications that can lead to less predictable, but potentially much more rewarding findings – or it may even "prevent" discoveries. This tendency is being fought. In the past, the OPC has indeed given time to novel, but risky projects, even if they occupied one of the large telescopes for about a week (as, for example, for an astroseismology investigation on α Cen A). Moreover, the OPC has given several months of observing time on a small telescope for an optical monitoring of the 1979 March 5 γ-ray burst error box. On the other hand, the OPC has also recommended extensive time for more routine studies. Thus, the small telescopes have been made available for an

Tentative Time-table of Council Sessions and Committee Meetings in 1986

October 3	Scientific Technical Committee, Venice
November 17–18	Finance Committee
November 18	Scientific Technical Committee
December 8–9	Observing Programmes Committee
December 11–12	Committee of Council

All meetings will take place at ESO in Garching unless stated otherwise.

In conjunction with the ESO-CERN Symposia on Cosmology and Fundamental Physics, CERN and ESO are organizing an

INTERNATIONAL SCHOOL ON ASTRO-PARTICLE PHYSICS

to be held at the "Ettore Majorana Centre for Scientific Culture", **Erice, Sicily, in the period 5–25 January 1987.** Co-sponsors are the Italian Ministry of Education, the Italian Ministry of Scientific and Technological Research, and the Sicilian Regional Government.

Recent progress in particle physics, cosmology and astrophysics has given birth to a new discipline that encompasses them all. These embryonic developments are not often covered in an interdisciplinary way. The purpose of this school is to fill this gap.

Lecturers will include J. Barrow, R. Brandenberger, B. Cabrera, A. de Rujula, L. Dilella, J. Ellis, J. S. Gallagher, G. Gelmini, D. C. Koo, L. Maiani, F. Melchiorri, D. V. Nanopoulos, K. A. Olive, B. E. J. Pagel, M. Rowan-Robinson, A. Sandage, R. Sanders, J. Silk, L. Stodolski, A. Szalay, F.-K. Thielemann, N. Turok, L. van Hove.

Persons wishing to attend the course should write to ASTROPARTICLE SCHOOL, TH Secretariat, CERN, 1211 Geneva 23, Switzerland, specifying date and place of birth, nationality, academic qualifications, list of publications, and present position. The total fee, including full board and lodging, is SF 1,400. Partial financial support can be provided in some cases, where the need is clearly justified. **The closing date for applications is 1 November 1986.**

efficiently organized, collective study of long-term photometric variables.

In summary then, the OPC only rarely specifically rejects an Application, and then only because of obvious faults. In general its procedures lead to selection by ranking: given the observing time available, only the best Applications can be accommodated. Furthermore, the OPC Members make a conscious effort to seriously consider innovatory, but risky proposals – even if they are rather time-consuming. All the time, measures are taken to minimize bias, at least in the long run.

Scheduling Observations

The actual scheduling of the best-ranked Applications on the various telescopes is done by ESO, immediately following the OPC Meeting. This is a complex task: many observing Applications propose the use of more than one telescope and focal-plane instrument, and other Applications have time constraints. Many multi-frequency investigations, for example, require the simultaneous use of other observatories on the ground or in space. And there are also single opportunities – stellar occultations, by planets or their moons, for example – that can only be observed in a single, predetermined night.

In addition, the schedule must be optimized, to avoid all-too frequent changes of focal-plane instruments on any one of the telescopes. This is a much more severe constraint than one would at first assume: in some cases it may result in no time being allocated to a well-rated programme.

The wide choice of auxiliary equipment that ESO offers on most of its telescopes requires grouping programmes that make use of the same instrumentation. This is necessary for efficient scheduling, because any exchange of focal-plane instruments brings a loss of observing time. In the case of infrared equipment at the 3.6 m telescope, for example, one loses a minimum of two nights: a special top end has to be installed and later on removed, both operations requiring delicate mechanical and optical adjustments. Consequently, such an instrument will not be mounted for one short observation, because the associated loss of telescope time to the community is of the same order as that gained for a single user.

Finally, the use of some detectors requires special technical assistance during the observations – and for infrared work this means night- and day-time assistance. Proper scheduling of the needed staff specialists then becomes an additional limiting factor. One will thus understand that, given all these limitations, the allotment of observing time can be a best compromise only.

The final Observing Schedule is approved by the Director General; he may occasionally make minor changes in order to redress extreme national imbalances. About two weeks after the OPC meeting, the applicants are informed about the outcome of their Applications and the observing Schedule is published.

Starting with Observing Period 38, negative replies to applicants may contain an indication on the OPC judgement of their observing proposals. There are three categories: "near", "below" and "far below the cutoff line". This scheme was introduced as the OPC's response to a wish expressed by many astronomers through the Users Committee.*

* The OPC, unfortunately, does not see a possibility to fulfil the repeatedly expressed wishes for a detailed justification of the ranking of all Applications. The OPC Members will, however, follow up inquiries by applicants from their country on a case-by-case basis.

It is hoped that prospective telescope users can see from the above description that considerable peer-pressure – becoming manifest in the OPC Meetings – forces the Members to do their homework conscientiously, judiciously and honestly; and that the OPC concentrates on scientific issues exclusively. In fact, this is probably the most striking aspect of the OPC Meetings. It certainly does impress new Members.

Undoubtedly, the OPC bears a heavy responsibility towards the community and, accordingly, the work of the OPC Members is very challenging and interesting. The present workload of the Members is close to the acceptable limit, though: if the semiannual two-day meetings are included, the time a Member spends on OPC work easily reaches three weeks or even a full month every year!

The OPC will always aim to maintain a standard of excellence in Observing Programmes. But ultimately, the OPC's success only manifests itself in a healthy, vigorous and successful research in all parts of the ESO community.

Visiting Astronomers

(October 1, 1986 – April 1, 1987)

Observing time has now been allocated for Period 38 (October 1, 1986 – April 1, 1987). As usual, the demand for telescope time was again much greater than the time actually available.

The following list gives the names of the visiting astronomers, by telescope and in chronological order. The complete list, with dates, equipment and programme titles, is available from ESO-Garching.

3.6-m Telescope

October 1986: Shaver/Clowes/Iovino, Mighell/Butcher/Buonanno/Gathier, Jörsäter/Bergvall, Bergeron/D'Odorico, Magain, Spitze F./Spite M./François, Heber/Hunger, Véron, Pickles/van der Kruit.

November 1986: Pickles/van der Kruit, Fort/Mathez/Mellier/Picat/Soucail, Chincarini/Manousoyannaki, Moorwood/Oliva, Danziger/Oliva/Moorwood, Rodriguez/Moorwood/Stanga, Israel/Koornneef, Reipurth/Le Bertre, Natta/Hunt/Vietri, Schulte-Ladbeck/Becker/Appenzeller/Leitherer, Marano/Zitelli/Zamorani, Nesci/Perola, Colina/Fricke/Kollatschny/Pérez-Fournon.

December 1986: Colina/Fricke/Kollatschny/Pérez-Fournon, Danziger/Rosa/Matteucci, Lequeux/Azzopardi/Comte, Lequeux/Azzopardi/Maeder/Mathys, Kudritzki/Humphreys/Groth/Butler/Steenbock, de Loore/David/Hensberge/Verschueren/Blaauw, Cristiani/Barbieri/Iovino/Nota, Krautter/Baade, Martinet/Jarvis/Pfenniger/Bacon.

January 1987: Martinet/Jarvis/Pfenniger/Bacon, Pakull/Angebault/Bianchi/Beuermann/Motch, Tanzi/Bouchet/Falomo/Maraschi/Treves, Westerlund/Petterson, Moneti/Natta/Stanga, Zadrozny/Leggett/Perrier, Léna/Leger/Mariotti/Perrier, Meisenheimer/Röser, Meisenheimer/Fugmann, Cristiani/Barbieri/Iovino/Nota, Röser/Meisenheimer, Grosbøl/Brosch/Greenberg, Bignami/Caraveo/Vigroux.

February 1987: Bignami/Caraveo/Vigroux, D'Odorico/Pettini, di Serego Alighieri/Tadhunter, Rodonò/Cutispoto/Ambruster/Haisch/Butler/Scaltriti/Vittone, Hessman/Mundt, Gratton/Ortolani, Wampler, Danziger/Fosbury/Gathier, Danziger/Dalgarno, Danziger/Fusbury/Tadhunter, Danziger/Binette/Matteucci.

March 1987: Danziger/Binette/Matteucci, Jarvis/Martinet, Schmutz/Hamann/Hunger/Wessolowski, Dennefeld/Désert, Israel/van Dishoeck, Stanga/Garay/Moorwood/Oliva/Rodriguez, Pottasch/Mampaso/Manchado, Röser/Meisenheimer, Bergeron/Boissé.

2.2-m Telescope

October 1986: Mighell/Butcher/Gathier/Buonanno, Franx/Illingworth, di Serego Alighieri/Shaver/Cristiani/Perryman/Bergeron/Macchetto, Perryman/Jakobsen, Schulz/Rafanelli/di Serego Alighieri.

November 1986: Surdej/Swings/Magain/Courvoisier/Kühr/Djorgovski, Grewing/Barnstedt/Nerri/Bianchi/Lenhard, Prangé/Gérard/Paresce/Vidal-Madjar, Paresce/Burrows/Vidal-Madjar/Lamers/Waters, Jakobsen/Perryman.

December 1986: Jakobsen/Perryman, Fusi Pecci/Buonanno/Corsi/Renzini, Melnick/Terlevich/Moles, Rodriguez/Binette, Stahl/Wolf/Zickgraf, Sommer-Larsen/Christensen, Martinet/Jarvis/Pfenniger/Bacon, Meylan/Djorgovski, Bertola/Zeilinger.

January 1987: Bertola/Zeilinger, Fricke/Hartmann/Loose, Westerlund/Pettersson, Dennefeld/Bottinelli/Gouguenheim/Martin/Le Squeren, de Bruyn/Stirpe, Bässgen M./Bässgen G./Grewing/Bianchi, Seitter/Duerbeck, Reipurth, Ulrich/Iye/Perryman, Jakobsen/Perryman, Vio/Barbieri/Cristiani, Tarrab/Kunth/Arnault/Vigroux/Prieto/Wamsteker.

February 1987: Tarrab/Kunth/Arnault/Vigroux/Prieto/Wamsteker, Keel, Seitter/Duerbeck.

March 1987: Ilovaisky/Chevalier/Angebault/Mouchet/Pedersen, Dettmar/Wielebinski, Labhardt/Spaenhauer, Lyngå/Gustafsson.

1.5-m Spectrographic Telescope

October 1986: Cacciari/Clementini/Malagnini, Bues/Rupprecht, Wagner/Appenzeller, Viton/Prévot/Sivan.

November 1986: Viton/Prévot/Sivan, Herczeg/Pietsch, Kubiak/Seggewiss, Geyer/Stepien/Mekkaden, Kubiak/Seggewiss, Pallavicini/Cerruti-Sola/Pasquini, Waelkens/Lamers/Waters/Le Bertre, Natta/Hunt/Vietri, Lub/de Ruiter, Wolf/Baschek/Scholz/Krautter/Reitermann.

December 1986: Wolf/Baschek/Scholz/Krautter/Reitermann, Heydari-Malayeri/Testor, Alloin/Pelat/Phillips, Acker/Stenholm/Lundström, Alloin/Pelat/Phillips, Lundgren, Alloin/Pelat/Phillips.

January 1987: Alloin/Pelat/Phillips, Focardi/Merighi, Tanzi/Bouchet/Falomo/Maraschi/Treves, Thé/Westerlund/Pérez, Haug/Drechsel/Strupat/Böhnhardt/Herczeg, Duerbeck, Courvoisier/Bouchet, Reipurth/Le Bertre.

February 1987: Reipurth/Le Bertre, Bender/Möllenhoff, Alloin/Pelat/Phillips, Lodén LO/Sundman, Kohoutek/Günter, Waelkens/Lamers/Waters/Le Bertre, Alloin/Pelat/Phillips, Pottasch/Pecker/Karoji/Sahu, Alloin/Pelat/Phillips.

March 1987: Alloin/Pelat/Phillips, Courvoisier/Bouchet, Schmutz/Hamann/Hunger/Wessolowski, Alloin/Pelat/Phillips, Lagerkvist/Hahn/Magnusson/Rickman, Schmutz/Hamann/Hunger/Wessolowski, Lagerkvist/Hahn/Magnusson/Rickman, Cox/Leene, Pastori/Antonello/Mantegazza/Poretti, Mantegazza, Magain, Alloin/Pelat/Phillips, Gerbaldi.

1.4-m CAT

October 1986: Foing/Beckman/Castelli/Crivellari/Vladilo, Crivellari/Foing/Beckman/Arribas/Castelli/Vladilo, Lindgren/Ardeberg/Maurice/Lundström, Didelon, Solanki/Mathys, Spite M./Spite F., Cayrel de Strobel.

November 1986: Cayrel de Strobel, Nissen/Andersen/Edvardsson/Gustafsson, Ferlet/Vidal-Madjar/Gry/Laurent/Lallement, Pallavicini/Cerruti-Sola/Pasquini, Ferlet/Vidal-Madjar/Gry/Laurent/Lallement, Vidal-Madjar/Ferlet/Lagrange, Rodonò/Catalano S./Cutispoto/Linsky/Neff, Ferlet/Vidal-Madjar/Lagrange, Martin/Maurice.

A Workshop organized by ESO on

STELLAR EVOLUTION AND DYNAMICS IN THE OUTER HALO OF THE GALAXY

will be held at ESO, Garching, **April 7–9, 1987.**

Topics of this 3-day workshop will include observational and theoretical aspects concerning chemical evolution and dynamics of field stars, globular clusters and planetary nebulae in the halo of our Galaxy and in halo systems – Magellanic Clouds and Dwarf Spheroidals.

More information may be obtained from M. Azzopardi at ESO, Karl-Schwarzschild-Str. 2, D-8046 Garching bei München, FRG.

December 1986: Maurice/Martin, Wolf/Zickgraf/Stahl, Barbuy, Barbuy/Arnould/Jorissen, Waelkens, Lenhart/Grewing, Gustafsson/Vilhu/Edvardsson.

January 1987: Gustafsson/Vilhu/Edvardsson, Bandiera/Focardi, Bouvier/Bouchet, Bandiera/Focardi, Bouvier/Bouchet, Bandiera/Focardi, François/Spite M., Baade/Peters/Polidan.

February 1987: Baade/Peters/Polidan, François/Spite M., Dachs/Hanuschik, Pottasch/Sahu, Ferlet/Vidal-Madjar/Lamers/Waelkens, Vladilo/Beckman/Crivellari/Molaro.

March 1987: Vladilo/Beckman/Crivellari/Molaro, Lanz/Mégessier/Landstreet, Gillet/Pelat, Magain, Brandi/Swings/Gosset, Stahl/Baade.

1-m Photometric Telescope

October 1986: Bues/Rupprecht, Liller/Alcaino, Kroll/Catalano F., Waelkens/Lamers/Waters/Le Bertre, Bergvall/Johansson, Guarnieri/Clementini/Fusi Pecci.

November 1986: Guarnieri/Clementini/Fusi Pecci, Labhardt/Spaenhauer/Trefzger, Collmar/Brunner/Kendziorra/Staubert, Chini/Krügel, Boisson/Balkowski/Durret/Rocca, Waelkens/Lamers/Waters/Le Bertre, Richtler/Spite M.

December 1986: Richtler/Spite M., Kohoutek/Steinbach, Bouvier/Bouchet, Waelkens/Lamers/Waters/Le Bertre.

January 1987: Westerlund/Pettersson, Mantegazza/Antonello/Conconi, Haug/Drechsel/Strupat/Böhnhardt/Herczeg, Waelkens/Lamers/Waters/Le Bertre, Reipurth, Waelkens/Lamers/Waters/Le Bertre, Poulain/Nieto/Prugniel, Grosbøl/Brosch/Greenberg.

February 1987: Grosbøl/Brosch/Greenberg, Thé/Westerlund/Perez, Waelkens/Lamers/Waters/Le Bertre, Rodonò/Cutispoto/Ambruster/Haisch/Butler/Scaltriti/Vittone, Dachs/Hanuschik, Magain, Waelkens/Lames/Waters/Le Bertre, Dreier/Barwig/Schoembs.

March 1987: Dreier/Barwig/Schoembs, Stanga/Moneti/Natta/Lenzuni, Waelkens/Lamers/Waters/Le Bertre, Lorenzetti/Ceccarelli/Saraceno, Epchtein/Nyuyen-Q-Rieu/Le Bertre, Waelkens/Lamers/Waters/Le Bertre, Di Martino/Zappala/Farinella/Cellino, Antonello/Conconi/Mantegazza/Poretti, Lyngå/Gustafsson, Gerbaldi.

50-cm ESO Photometric Telescope

October 1986: Group for Long Term Photometry of Variables, Geyer/Stepien/Mekkaden.

November 1986: Geyer/Stepien/Mekkaden, Carrasco/Loyola, Rodonò/Catalano S./Cutispoto/Linsky/Neff, Group for Long Term Photometry of Variables.

December 1986: Group for Long Term Photometry of Variables, Bouvier/Bouchet.

January 1987: Bouvier/Bouchet, Lindgren/Ardeberg/Maurice/Prévot/Lundström, Carrasco/Loyola, Thé/Westerlund.

February 1987: Thé/Westerlund, Thé/Westerlund/Pérez, Rodonò/Cutispoto/Ambruster/Haisch/Butler/Scaltriti/Vittone, Kohoutek/Günter, Lagerkvist/Hahn/Magnusson/Rickman.

March 1987: Lagerkvist/Hahn/Magnusson/Rickman, Carrasco/Loyola, Scaltriti/Busso.

GPO 40-cm Astrograph

October 1986: Scardia.

November 1986: Scardia.

February 1987: Debehogne/Machado/Caldeira/Vieira/Netto/Zappalà/De Sanctis/Lagerkvist/Mourão/Protitch-Benishek.

March 1987: Debehogne/Machado/Caldeira/Vieira/Netto/Zappalà/De Sanctis/Lagerkvist/Mourão/Protitch-Benishek.

1.5-m Danish Telescope

October 1986: Leibundgut/Tammann, Ulrich/Iye, Giraud.

November 1986: Prévot/Viton/Sivan, Grenon/Mayor, Trefzger/Mayor/Pel, van Paradijs/Mayor/Verbunt/Zwaan, Schulte-Ladbeck/Becker/Appenzeller/Leitherer, Melnick/Terlech/Moles.

December 1986: Melnick/Terlevich/Moles, Nørgaard-Nielsen/Hansen/Jörgensen, Valentijn/Lauberts/Peletier.

January 1987: Lindgren/Ardeberg/Maurice/Prévot/Lundström, Andersen/Nordström/Olsen, Larsson, Brinks/Klein/Danziger/Matteucci.

February 1987: Brinks/Klein/Danziger/Matteucci, Fusi Pecci/Bonifazi/Romeo/Foardi/Buonanno.

March 1987: Mermilliod/Mayor/Andersen/Nordström, Mayor/Duquennoy/Andersen/

Nordström, van Paradijs/van der Klis, Ilovaisky/Chevalier/Angebault/Mouchet/Pedersen.

50-cm Danish Telescope

November 1986: Kubiak/Seggewiss, Sterken/vander Linden.
December 1986: Sterken/vander Linden.
January 1987: Lodén K., Lindgren/Ardeberg/Maurice/Prévot/Lundström.

90-cm Dutch Telescope

October 1986: Gautschy, Schneider/Weiss.
November 1986: van Paradijs/Mayor/Verbunt/Zwaan, Trefzger/Pel/Blaauw.
December 1986: Trefzger/Pel/Blaauw, Lub/de Ruiter, de Loore/David/Blaauw/Verschueren/Hensberge.
January 1987: de Zeeuw/Lub/de Geus/Blaauw, v. Amerongen/v. Paradijs, Grenon/Lub.
February 1987: Grenon/Lub.
March 1987: Waelkens/Heynderickx.

61-cm Bochum Telescope

October 1986: Weiss/Schneider, Bianchi/Cerrato/Grewing/Scales.
November 1986: Bianchi/Cerrato/Grewing/Scales, Kohoutek/Steinbach.
December 1986: Kohoutek/Steinbach.

Hunting Halley's Comet

W.E. CELNIK, Astronomisches Institut, Ruhr-Universität, Bochum, FRG

Observers of bright comets have always been fascinated by the sight of these rare phenomena. However, it was as late as the 19th century that scientists started to make systematic observations of the appearance of comets and recorded them in the form of drawings and descriptions of comas and tails. Halley's comet in particular was observed intensively because the time of its return was well known. The first photographic observations of the comet were made during its 1910 perihelion. A large number of photographs were taken using astronomical instruments of all dimensions showing structures within the extended ion tail and the bright coma. Pictures from that time are well suited to be compared with recently obtained images of the 1986 appearance, although observing conditions were then much less favourable. Just when P/Halley was most active, at its brightest, and thus most interesting, namely during its perihelion passage, it was behind the Sun and unobservable. During the 2,000 years that observations of this comet have been recorded, there was only one appearance where the positions of Sun, Earth and comet were even worse for observations. In addition, the observing conditions in the northern hemisphere were extremely bad because at its best time the comet followed its path through the southern skies. Thus the only way to observe P/Halley successfully after its perihelion passage was to got to the southern hemisphere. At a latitude of 30 degrees south the comet culminated near the zenith.

Figure 1: *Comet P/Halley in the morning twilight of February 22, 1986, 9 : 01 UT from La Silla. Camera 1 : 2/110 mm, filter OG 530, IIIa–F hypersensitized, exposure time 3 minutes.*

The author and some colleagues from the Astronomical Institute of the Ruhr University in Bochum (FRG) were very interested in observations of P/Halley. Although solar system bodies are not the main field of work in our institute, a new small study group was set up to prepare, implement and evaluate observations of this comet. Collaborators are P. Koczet, Prof. W. Schlosser, R. Schulz, K. Weissbauer and the author. This was in February 1985, exactly 12 months before the approximation of P/Halley to the Sun. Thus time was short. A scientific observing programme demands extensive deliberation and preparation in order to produce new knowledge about the object. An important question was how to finance the campaign. Towards the end of June 1985 an application to the "Deutsche Forschungsgemeinschaft" was made for financial support of the project. This support was granted in September 1985. Now there was only little time left to acquire all the necessary instruments and equipment because we wanted to start the observations as early as possible after the perihelion which was on February 9, 1986. It was decided to restrict the campaign to photographic photometry and the investigation of structures in the coma and tail of P/Halley.

Determination of the brightness distribution across coma and tail is only valid if certain components of cometary matter are considered. Thus four wide-field cameras were used to take plates simultaneously in the light of the neutral CN molecule at 3880 Å wavelength using an interference filter of 50 Å bandwidth, in the light of the ionized CO^+ molecule at 4260 Å (filter bandwidth 100 Å), of the dust tail using a long-wave pass filter at 5300 Å, and of the ion tail with a filter combination resulting in a spectral range from 3750 to 4500 Å. To obtain a field of view of 30 degrees we used cameras of the format 6 × 6 cm and 6 × 6 objectives of the focal length 110 mm and a focal ratio of f/2. For the photographic emulsion we chose fine-grain hypersensitized IIIa–F. The optical filters for the wide-field images have a diameter of 65 mm and were set in front of the optics.

In order to study the structures within the cometary coma with high spatial resolution, we acquired a Flat-Field Camera 1 : 4/760 mm with a field of view of 1.8 × 2.7 degrees if 35 mm film is used. This instrument too was equipped with optical filters to obtain images in CN, CO^+ and of the dust coma. Photographs with this camera were taken with 103a–E, a–F and TP 2415 35 mm film, all hypersensitized.

From an amateur we bought a used but very stable parallactic mounting which is controlled by stepping motors in both right ascension and declination. Velocities in both directions were adjusted to follow the comet automatically as well as possible. A refractor with focal length 1,000 mm and f/10 served as a guiding telescope. It was modified to give an enlargement of 150–200 × and a field of view of 25 arcminutes.

The location of our observations was the ESO observatory at La Silla where our institute has a telescope of its own (diameter 61 cm, f/15) and where a complete infrastructure exists. There the comet could be observed optimally and

Figure 2: *Comet P/Halley on March 10, 1986, 8 : 26 UT from La Silla. Camera 1 : 2/110 mm, filter IF λ 4260, IIIa–F hypersensitized, exposure time 110 minutes.*

Figure 3: *Comet P/Halley on April 17, 1986, 2 : 00 UT from La Silla. Camera 1 : 2/ 110 mm, filter IF λ 4260, IIIa–F hypersensitized, exposure time 100 minutes.*

the Bochum telescope could be used for photometric parallel measurements. We are very grateful to ESO for granting us this possibility although our application for it was somewhat late. We thank especially the Director General, Prof. Woltjer, Mr. Schuster, Mr. Hofstadt, Mr. Bauersachs and Mr. Perez for their support.

On February 12 we arrived at La Silla coming from icy Europe; the temperature difference was 40 degrees. After setting up our equipment not far from the 61-cm telescope we observed P/ Halley photographically for the first time on February 17 in the bright morning sky in the light of CN. Some days later the tail had developed so well that it could be observed easily with the naked eye. On February 22 we detected a double ion tail and six well-separated dust tails. The opening angle of the whole tail increased to more than 160 degrees. This multiple tail was a result of some isolated eruptions of gas and dust from the cometary nucleus. The maximum tail length visible to the naked eye was approximately 15 degrees; on the wide-field images the ion tail was sometimes longer than 25 degrees. One of the most interesting phenomena can be seen in the image of the CO^+ tail from March 10. It is a so-called disconnection event. Reasons for this event are still not completely understood. Perhaps the Bochum Halley campaign can help to solve this problem. At the beginning of April the comet moved along its path through the galactic disk – a very impressive sight but a handicap for the investigation. The surface brightness of the Milky Way in the background was partly higher than that of the comet tail and disturbs the interpretation of the images taken at that time. By mid-April, ion and dust tail of P/Halley had very well separated. They pointed to directions differing by approximately 90 degrees, a result of the altered geometry between Sun, Earth and comet.

During a total of 60 observing nights from February 17 to April 17, we were able to obtain more than 1,200 images of the comet in four different spectral ranges, most of them being of high quality. Exposure times lay between 10 seconds and 170 minutes. These images are now being analysed in Bochum with regard to two aspects: (1) investigation of the dynamics in coma and tail and the connections to the rotational period of

Figure. 4: *Comet P/Halley on March 16, 1986, 7 : 02 UT from La Silla. Flat-Field Camera 1 : 4/760 mm, filter OG 530, 103a–F hypersensitized, exposure time 15 minutes.*

Figure 5: *Comet P/Halley on March 16, 1986, 7 : 56 UT from La Silla. Flat-Field Camera 1 : 4/760 mm, filter IF λ 4260 (CO⁺), 103a–F hypersensitized, exposure time 60 minutes.*

Figure 6: *Comet P/Halley on March 16, 1986, 9 : 15 UT from La Silla. Flat-Field Camera 1 : 4/760 mm, filter IF λ 3880 (CN), 103a–F hypersensitized, exposure time 60 minutes.*

Figure 7: *Comet P/Halley near the radio galaxy NGC 5 128 on April 15, 1986, 1 : 22 UT from La Silla. Flat-Field Camera 1 : 4/760 mm, filter GG 410, 103a–E hypersensitized, exposure time 20 minutes.*

the nucleus and the reactions with the solar wind, and (2) determination of abundances, production rates, and lifetimes of certain molecules as a function of the heliocentric distance of the comet. But these procedures are expected to take some time . . .

(Further information about the Bochum Halley campaign has been given in *Sterne und Weltraum* **25,** pages 221 (4/1986), 280 (5/1986) and 298 (7–8/1986).

Spectroscopy, Photometry and Direct Filter Imagery of Comet P/Halley

C. ARPIGNY, F. DOSSIN, J. MANFROID, Institut d'Astrophysique, Université de Liège, Belgium,
P. MAGAIN, ESO
A. C. DANKS, Department of Physics and Astronomy, Michigan State University
D. L. LAMBERT, McDonald Observatory and Department of Astronomy, University of Texas, Austin, and
C. STERKEN, Vrije Universiteit Brussel

The return of Comet P/Halley, as well as the related space missions, added to the intrinsic interest of comets and their importance in connection with the cosmogony of the Solar System, no doubt explain the high level of activity devoted to the study of these celestial bodies in recent years. While considerable progress has been achieved in this field, thanks to the use of new observational techniques and to numerous theoretical works, we are forced to admit that quite a long way remains ahead before a satisfactory understanding of the nature and origin of comets is to be reached. The unique opportunity offered by Comet Halley to gather an unprecedented wealth of original data of all kinds has given rise to a truly worldwide mobilization and we in Liège wanted very much to participate in this remarkable enterprise, in view of the continued interest shown by our institute in cometary physics and spectroscopy, ever since Professor Swings' pioneering work. When it was realized that our plans had so much in common with those of our colleagues from the Universities of Michigan, Texas, and Brussels, we decided all together to join our efforts.

The principal aim of our programme is to derive some information on the physical characteristics of the cometary atmosphere (distribution laws of densities, temperature and velocity as functions of the distance to the nucleus) by analyzing in detail the relative intensities of the molecular emissions, their variation with the position on the comet's image, as well as the evolution of these properties as the distance from the Sun, r, changes. The procedure followed to interpret the relative intensity distributions is to construct synthetic spectra integrating through the coma and taking into account radiative processes (resonance-fluorescence excitation by the solar radiation, sensitive to the radial velocity of the molecules relative to the Sun – the so-called "Swings effect") as well as collisional effects which may be

significant in the innermost regions (Arpigny, 1976). The modelling of the structure of the coma indeed represents a necessary step towards the ultimate goal of the study of comets, namely the determination of the chemical composition of the basic material in the nucleus.

We have selected a number of specific observations or special problems related to this general programme and we shall outline these briefly here, grouping them according to the various instruments we used at La Silla during the post-perihelion phase of Comet P/Halley, essentially from mid-March to the beginning of June 1986.

1.5-m Telescope Coudé Spectrograph

One appreciable advantage offered by this instrument is the possibility to use a rather long slit (approximately 3.5 arcminutes) and hence to study the variation of the spectral intensity distributions over a fairly large projected distance (ϱ), a feature essential to the construction of model cometary atmospheres. Thus, radial profiles B (ϱ), i.e. the distributions of the surface brightness along a diameter of the apparent cometary disk, can be established for the various species. Assuming negligible optical thickness, which is valid in most cases, this gives also the column densities N (ϱ) and these, when compared with the profiles predicted by the models, should yield clues relevant to the production mechanisms of the observed radicals. For the same reason, possible spatial variations of the ionic emissions related to the accelerations of the carriers, OH^+, CO^+, CH^+ . . . ("Greenstein effect") can be searched for, which may throw some light on a long-standing enigma: "bulk versus wave motions in the plasma tail". Besides, observations with this configuration will allow a direct comparison with similar spectra secured with the twin 1.5-m telescope at the Haute-Provence Observatory (HPO) on several comets, notably on Bennett (1970 II). It will also be possible to relate these observations to a series of pre-perihelion spectra of P/Halley taken by some of us at HPO from the middle of November 1985 to the beginning of January 1986.

Approximately three hours exposures, one on each night, from 15 to 18 March produced three good spectra in the blue, and one rather weak in the visual spectral region. The best spectrogramme, covering the range from the NH (0,0) band to the C_2 Swan (0,0) band is reproduced in Figure 1. The orientation of the slit was in the general anti-solar direction, while the telescope was guided in such a way as to keep the central part of the comet near the sunward end of the slit. As a result, the tail emissions show up quite well and are seen over about 125,000 km. The extreme weakness of the solar radiation scattered by the dust tail also makes the identification of some of the molecular tail emissions easier than in the case of Comet Bennett, for example. Especially noteworthy are: (a) the well-known CO^+ Comet-Tail bands and several bands due to the Fox-Duffendack-Barker System of CO_2^+, indicating a CO_2^+/CO^+ ratio somewhat higher in P/Halley near r = 0.95 A.U. than in Bennett at comparable heliocentric distances; the CO_2^+ bands are $^2\pi-^2\pi$ doublets and here as in a number of other comets (see Festou et al., 1982), the 1/2–1/2 component is systematically stronger than the 3/2–3/2 component in the various bands, for some unknown reason (we have verified that this peculiar coincidence is not a Swings effect associated with the comet's orbital velocity); (b) the OH^+ (0,0) and (0,1) bands, the latter identified for the first time; furthermore, the (1,0) band of this ion may have some weak contribution near the short-wavelength edge of the NH (0,0) band; (c) the CH^+ (0,0) and (1,0) bands, a few lines of which are also seen for the first time; (d) some fairly strong ionic features at 371.48, 372.79, 410.95, 412.34, 414.59, and 416.01 nm, for which we have not found any satisfactory assignment.

Figure 2 illustrates at higher magnification a particularly rich section, 390–430 nm, from the same spectrum, where we can appreciate the remarkable spectral definition, in the CO^+ and CN bands. The quality achieved undoubtedly pleads for maintaining this instrument, which can still provide quite valuable data indeed. This material will enable us to carry out elaborate studies of the rotational intensity distributions of the various molecular bands.

1.4-m CAT, Coudé Echelle Spectrometer, Reticon

There are quite a few very important problems on which progress is possible only thanks to high-resolution observations (of the order of one hundredth of a nanometer). In this category we have chosen to try and evaluate the isotopic abundance ratio $^{12}C/^{13}C$, which was given high priority in our cooperative project.

This ratio changes depending on the degree of nuclear processing that has taken place and a wide range of values is seen in different astrophysical sites, from ~89 in the Solar System to ~25 in the Galactic Centre, down to ~5 in some late-type stars. Knowledge of its value in comets is of great interest in connection with the origin of these bodies. Now this question of how, when and where comets were formed is still a matter of animated discussions. Various hypotheses envisage that they originated within the Solar Nebula, just beyond the Uranus-Neptune zone, or further out, 10^3 to 10^4 A.U. from the centre, or at the outskirts, in associated disks or fragments of the Nebula, or else in interstellar clouds from which they were captured by the Sun. Whatever their birthplaces, the determination of their isotopic (and chemical) composition will have implications upon the history of the Solar System, upon the conditions in an interstellar cloud, or eventually even upon some of our ideas concerning star formation. That comets

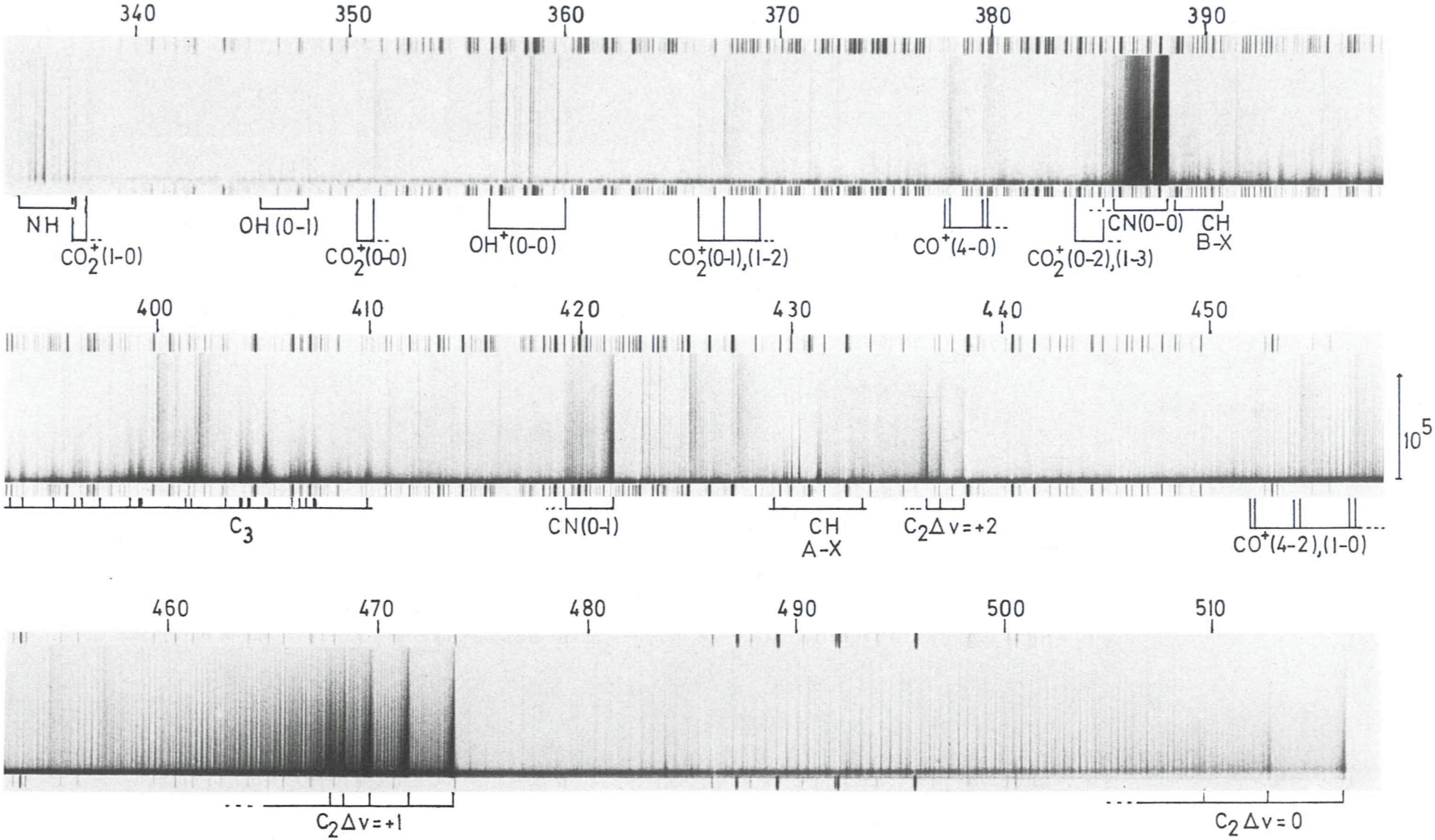

Figure 1: *Spectrum of Comet·P/Halley (r = 0.96 A. U.) obtained with the coudé spectrograph at the 1.5-m telescope (sensitized IIa–O emulsion; original reciprocal dispersion 20 Å/mm; exposure time 3 h 25 min). The continuous strip at the bottom is due to the scattering of the solar radiation by small solid particles forming a halo around the nucleus. The tail of the comet is in the upward direction; the angle between its axis and the slit of the spectrograph varied from 55° to 5° during the exposure. The rotational structure of the various molecular emissions is well resolved thanks to the remarkable optical quality of this spectrograph. The vertical bar on the right represents 10^5 km projected on the comet.*

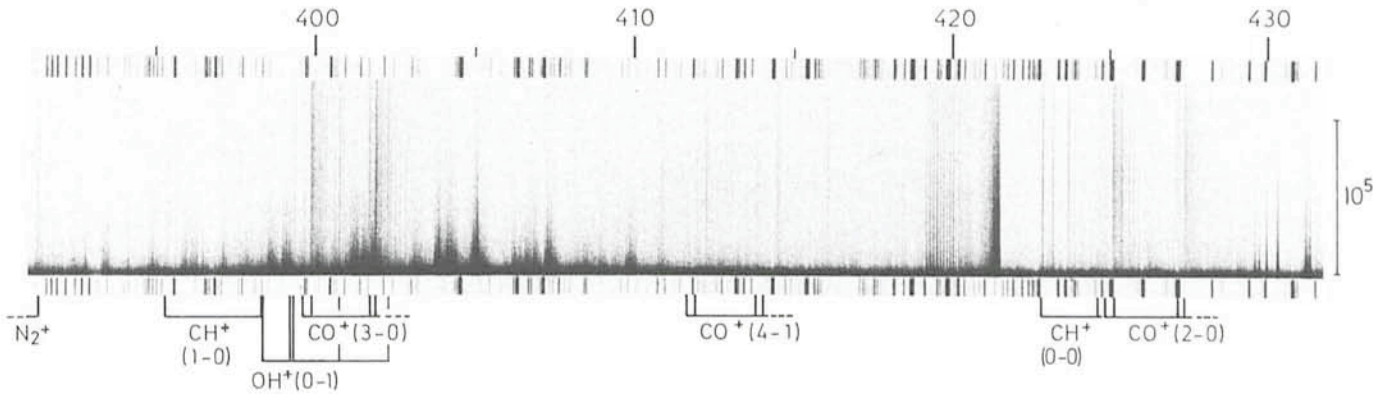

Figure 2: *Enlarged section from the spectrum appearing in Figure 1. For the sake of clarity, only the ionic emissions in this region are identified here, the neutral emissions in the same region being marked in Figure 1.*

may be regarded as primitive, essentially unfractionated bodies is due to their very long stay in very cold environments far from the Sun as well as to their very small mass, typically $\sim 10^{14}$ kg.

Measurements of the carbon isotopic ratio have been performed in half a dozen comets so far generally using the C_2 (1,0) Swan band. The Swan system is strong in comets and the 473.7 bandhead would in principle offer easy measurement of the $^{12}C/^{13}C$ ratio, as the introduction of the ^{13}C atom shifts the isotopic bandhead to 474.5 nm. Unfortunately, however, the $^{12}C^{13}C$ (1,0) bandhead happens to be severely blended with NH_2 features, which makes the extraction of the isotopic ratio rather delicate (Danks et al., 1974). In Comet West (1976 VI) another candidate, the C_2 (0,0) band, was tried. This band is appreciably stronger but has a much smaller isotopic shift; in that case, one has to look at individual rotational lines rather than at a bandhead and it turns out that very weak satellite lines of the normal $^{12}C_2$ molecule must be separated out (Lambert and Danks, 1983). Values from ~ 135 to ~ 50 with quite large error bars have been found for $^{12}C/^{13}C$ in the comets studied so far (see e.g. Danks, 1982).

We attempted to repeat these observations on Comet Halley with the CES, which provides the very high resolving power necessary to disentangle or at least reduce the blending problems involved here. Several trials on the C_2 (1,0) bandhead proved disappointing, the comet being fainter than anticipated. Thus we decided to concentrate upon the C_2 (0,0) band near 516 nm, the brightest emission in the visible. One single exposure of about one hour at a resolution of ~ 0.005 nm revealed the rotational structure of the band, however the intensities of the $^{12}C^{13}C$ lines are very low, of the order of 1 % those of the corresponding $^{12}C_2$ features, so that repeated measurements were needed in order to bring these lines above the noise. Ten integrations were made in total (10 March, 23–30 March; 45 to 60 minutes each, with resolutions of 80,000 to 100,000). One of these spectra is shown in Figure 3; this is one of the first and few spectra obtained on Comet Halley at this high resolution. It is also the first time such a resolution is used to record a molecular cometary spectrum. Let us hope there will be more opportunities of this kind on future bright comets! Naturally, from night to night Comet Halley was changing velocity, introducing a wavelength displacement in the observed bands. Therefore, before co-adding data, each image frame has to be shifted slightly.

To aid interpretation and to act as a reference source, we managed to persuade the TRS and Mr. Van Howard to illuminate the slit area with an acetylene torch. At the high temperature of the C_2H_2 torch we could produce the emission spectrum of C_2 which also exhibits the terrestrial ratio of $^{12}C/^{13}C$, ~ 89. These lines are useful for different reasons. In particular, they are not superimposed on the scattered solar continuum, as are the comet lines and on the other hand, their intensities are due to thermal excitation, whereas the comet lines are excited by the resonance-fluorescence mechanism. Elimination of the underlying continuum in the cometary spectrum is effected by dividing by a solar type spectrum. In our case the most convenient body was the planet Mars, of which several short exposures were made.

These observations were successful, given the comet's brightness, and reduction of the data is in progress. We should be able to give both a measure of the $^{12}C/^{13}C$ ratio and a value for the rotational temperature of C_2 in Comet Halley in the near future.

Another item in this part of our programme was concerned with the forbidden atomic oxygen lines already mentioned above. Indeed, the stronger, shortward component of the [OI] doublet is perturbed by HN_2 emissions at low resolution and the oxygen abundances

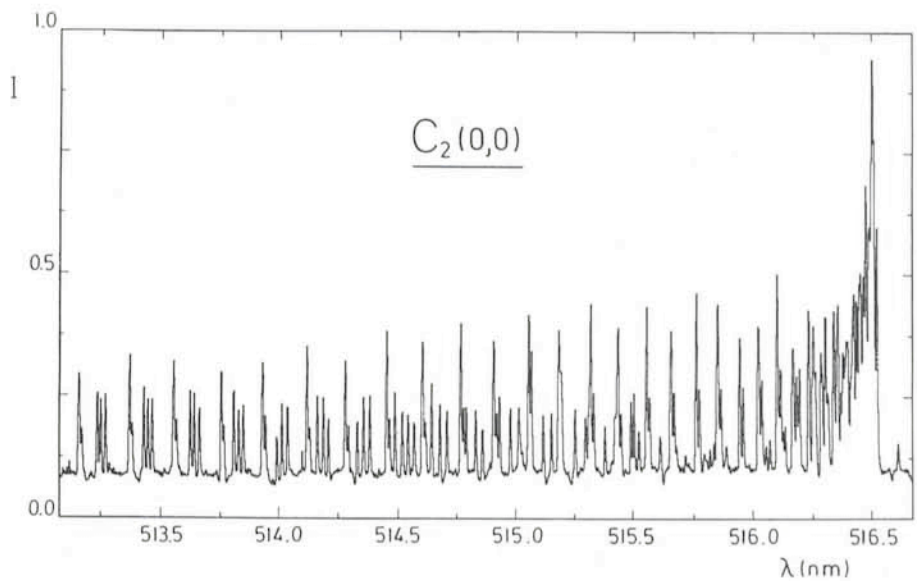

Figure 3: *The rotational intensity distribution in the C_2 (0,0) band of P/Halley (r = 0.85 A.U.) at 100,000 resolution (Coudé Echelle Spectrometer at the 1.4-m CAT).*

reported so far depend upon an assumption regarding the strength of these NH_2 emissions that needs to be checked by resolving the blend. We obtained eight spectra covering the range 628.5–633.5 nm (24 March, 5, 7, 8, 27 April; resolution 50,000); some of these were taken at different positions in the sunward and anti-sunward directions in order to study the mechanism by which the oxygen atoms are formed.

50-cm ESO Photometric Telescope

Photometry is also an efficient tool in cometary studies. A glance at a typical spectrum (see Fig. 1 and 2) shows that normal U, B, V or even intermediate bandpass photometry is of little help in such an intricate superposition of molecular emissions and solar continuum. To overcome these difficulties, special filters like those defined by the IAU have to be used. These filters have narrow bandpasses, typically a few nanometers. They isolate characteristic features such as the CN 387 nm emission, or a particular emission-free zone of the spectrum so that the continuum is readily accessible.

The advantages of photometric observations are the usual ones:
– accurate and relatively easy absolute calibration;
– simple and reliable instrumentation;
– fast observation;
– theoretical availability of a large number of telescopes, mainly of small size, all over the world (Europe being underrepresented in that respect).

Observations have been carried out at La Silla and in many other places, first of P/Giacobini-Zinner during the trial run of the IHW, and then of P/Halley. Diaphragms of different sizes are used in order to analyze the radial distribution of the various emissions. Combination of the observations made at different observatories, with a wide distribution in longitude, will eventually give an almost continuous monitoring of Comet Halley's activity both before and after perihelion.

Our first P/Halley observing run at La Silla was of 12 nights (27 March–7 April), when the comet was still relatively bright and moving swiftly in front of the Milky Way background. This stellar background proved to be a problem as it was not easy to evaluate the exact sky brightness affecting the comet measurements. One striking result of these observations was the important fluctuations exhibited by the comet, by factors of 2 or more, from one night to the next, in agreement with many other reports of such variability. In addition, on several nights a few hours were devoted to differential observations with a single diaphragm. Measurements were performed in quick succession alternatively of a comparison star and of P/Halley so that more rapid variations could be detected.

One difficulty arises from the limited choice of diaphragm sizes. Even small telescopes in the 0.5-m class rarely have diaphragms larger than 1 arcminute. For nearby objects this of course means small linear dimensions. Fortunately, the versatility of the ESO telescopes and in particular of the 0.5-m used for our study allowed to record the intensity in the various filters during radial scans across the coma. Figure 4 gives a few examples of such scans from the nucleus out to 5 arcminutes in the directions towards and away from the Sun. Thus the distribution of the different spectral contributions can be followed farther out and more accurately than with the classical method of multiple diaphragms.

During our second photometric observing period we were able to make one last set of measurements through all nine IAU-IHW filters (24 June).

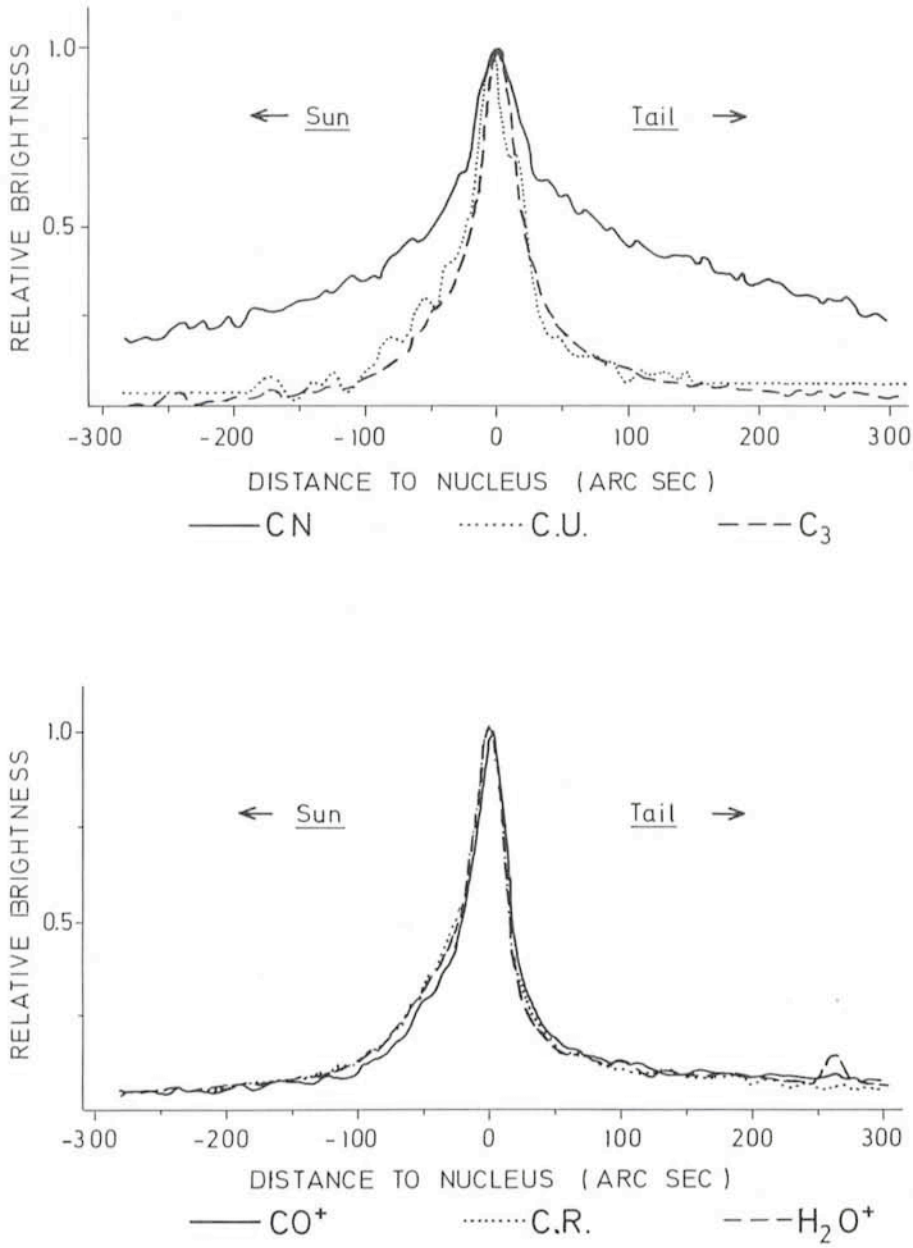

Figure 4: *Examples of photometric scans across P/Halley's coma along the Sun-antisun line, through various filters (C.U. = Ultraviolet continuum, 365 nm; C.R. = Red continuum, 684 nm). The asymmetry in the CN profile can probably be attributed to the effect of solar radiation pressure on radicals produced with a velocity dispersion. On the other hand, the asymmetry of opposite sign in the other molecular emissions, imitating the profiles in the continuum, seems to indicate contamination of these molecular emissions by scattered solar radiation.*

1.5-m Danish Telescope, CCD Camera

Having acquired a set of IHW imaging quality filters which isolate the same molecular emissions and continuum windows as the photometric filters (with the exception of the OH filter), we wanted to take advantage of the favourable conditions near the perigee of P/Halley and obtain high spatial resolution pictures. Thus a total series of about forty frames were secured on 8 and 9 April, when the geocentric distance of the comet was ~0.42 A.U. The exposure times ranged from 1 minute with the red filters to 10–20 minutes near 400 nm.

Now, the nearness of the comet to the Earth also has a drawback in that it causes a troublesome very rapid apparent motion of the object. Indeed, at a rate of some 16″/min the autoguiding system had a hard time in trying to follow the comet perfectly. Therefore we decided to split the longest exposures into several shorter ones in order to preserve the excellent spatial resolution (a few 100 km), the more so that the image quality itself was quite good (seeing ~0.″9). This will of course require delicate image processing. We hope to end up with valuable "monochromatic" bidimensional data, covering a field of about 45,000 × 70,000 km projected on the comet. The resulting spatial distributions of the various components may provide useful information bearing upon the enigmatic question of how they are produced in the inner coma.

Let us mention here that we were struck by the similitude between some of the pictures, especially the red ones, H_2O^+ and red continuum, suggesting that the solar radiation scattered by the dust may have a predominant contribution even in a filter centred on a molecular emission and that careful treatment will be necessary in order to derive significant results from images taken through such filters.

We all enjoyed living and working in a very hospitable and dynamic observatory and we appreciated very much the efficient help we received on many occasions in the course of our activities at ESO. Our heartiest thanks to all who contributed to make our respective stays in La Serena and in La Silla so pleasant and fruitful!

References

Arpigny, C.: 1976, Proc. IAU Coll. Nr. 25, "The Study of Comets", NASA SP-393 (Donn et al., eds.), 797–838.

Danks, A.C.: 1982, ESO Comet Halley Workshop, Paris (Véron, ed.), 155–170.

Danks, A.C. and Arpigny, C.: 1973, *Astron. Astrophys.* **29,** 347.

Danks, A.C., Lambert, D.L. and Arpigny, C.: 1974, *Astrophys. J.*, **194,** 745.

Festou, M.C., Feldman, P.D. and Weaver, H.A.: 1982, *Astrophys. J.* **256,** 331.

Johnson, J.R., Fink, U. and Larson, S.M.: 1984, *Icarus* **60,** 351.

Lambert, D.L. and Danks, A.C.: 1983, *Astrophys. J.*, **268,** 428.

Spinrad, H.: 1982, *Publ. Astron. Soc. Pac.* **94,** 1008.

The PHEMU 85 International Campaign

J.E. ARLOT[1], P. BOUCHET[2], CH. GOUIFFES[2], B. MORANDO[1], F.X. SCHMIDER[2], W. THUILLOT[1]

[1] *Bureau des Longitudes, Paris*
[2] *ESO, La Silla*

1. Introduction

The mutual phenomena of the Galilean satellites of Jupiter take place every six years, when the Earth and the Sun cross the equatorial plane of Jupiter which coincides with the orbital planes of the satellites. At that time, mutual occultations and eclipses may occur. However, the only favourable situation for observing such phenomena is when the crossing of the equatorial plane occurs simultaneously with the opposition of Jupiter. These phenomena are often observable only once every twelve years. In 1985, during the latest opposition of Jupiter, its declination was between −19 and −15 degrees, which made La Silla one of the best places to observe them.

In order to improve the theory of the motion of the Galilean satellites, two kinds of observations have been made so far: photometric observations of the eclipses by Jupiter yielding a positional accuracy of 1,000 km and photographic astrometry giving an accuracy of 300 km. However, as the satellites have no atmosphere, an even higher accuracy can be achieved by observing mutual phenomena, that are eclipses and occultations of the satellites by themselves. These observations are the most precise that can be made of those bodies and lead to a precision of about 100 km, which explains why international campaigns have been organized to carry them out.

Is such a precision for a position of the Galilean satellites necessary? The answer is yes for several reasons. First, the exploration of Jupiter and its satellites by space probes requires a very accurate knowledge of the orbital motions of these bodies. This will especially be the case when the Galileo probe in a few years will be put in orbit around Jupiter. Secondly, the motion of the Galilean satellites around Jupiter, affected by several so far little understood perturbations, is one of the most complex problems of celestial mechanics. The system of moons is submitted to very fast changes and by studying these we may hope to detect non-gravitational effects. Io, for instance, is suspected to have a secular acceleration due to energy dissipation. It is a very inconspicuous effect which cannot be observed easily, but observations of mutual phenomena over a couple of Jupiter oppositions should allow us to explore it.

Therefore, an international campaign, PHEMU 85, has been organized by the Bureau des Longitudes (France), bringing together theoreticians working in celestial mechanics and observational astronomers (which does not happen so often!). As part of this campaign, ESO allocated a large amount of observing nights to the programme at the ESO 50-cm and 1-m telescopes. In total we were able to observe 46 mutual phenomena, during 32 nights (or half-nights).

2. The Observations

The observations were carried out in fast photometry mode, generally with a time resolution of 50 ms. This mode of observing is briefly described in the present issue of the *Messenger* and has been extensively used already in the

TABLE 1

Date	Phenomenon	Observing conditions (a)	Result (b)	Telescope	Filter	Diaphragm
26/27. V .85	3.occ.1	1 – 2	0	50 cm	V	15″
28/29. V .85	2.occ.4	3	0 – 1?	50 cm	V	10″
29/30. V .85	2.occ.4	3	3	50 cm	V	10″
02/03. VI .85	3.occ.2	3	3	50 cm	V	10″
	3.occ.1	3	–	50 cm	V	10″
09/10. VI .85	3.occ.2	3	3	50 cm	V	10″
15/16. VI .85	1.occ.4	1	–	50 cm	V	15″
09/10. VII .85	3.occ.1	2	–	50 cm	V	10″
	4.occ.1	2 – 1?	3	50 cm	V	10″
11/12. VII .85	4.occ.3	2 – 1	1	50 cm	B	15″
15/16. VII .85	3.ecl.2	1	–	50 cm	V	20″
	3.occ.2	1	2	50 cm	V	20″
18/19. VII .85	1.occ.4	3	3	50 cm	V	10″
19/20. VII .85	1.occ.3	1	–	50 cm	V	10″
26/27. VII .85	1.occ.3	2	–	50 cm	V	10″
02/03. VIII.85	1.occ.3	3	3	50 cm	B	10″
05/06. VIII.85	3.occ.4	1	–	50 cm	V	10″
	3.occ.2	1	–	50 cm	V	10″
	3.ecl.2	1	–	50 cm	V	10″
09/10. VIII.85	1.occ.3	2 – 1	–	50 cm	V	10″
28/29. VIII.85	3.ecl.2	3	3	1 m	V	7″
	4.occ.1	3	3	1 m	V	7″
03/04. IX .85	3.occ.2	1	–	50 cm	V	10″
	3.ecl.2	1	–	50 cm	V	10″
04/05. IX .85	3.occ.2	3	3	50 cm	B	10″
05/06. IX .85	1.occ.4	1	–	50 cm	V	10″
	1.occ.4	1	–	50 cm	V	10″
07/08. IX .85	1.ecl.3	3	3	50 cm	B	10″
13/14. IX .85	1.occ.2	3	3	50 cm	B	15″
	1.ecl.2	3	3	50 cm	B	15″
	4.occ.2	3	0	50 cm	B	15″
14/15. IX .85	1.occ.3	3	3	50 cm	V	10″
	1.ecl.3	3	0	50 cm	V	10″
20/21. IX .85	1.occ.2	3	3	50 cm	B	15″
	1.ecl.2	3	3	50 cm	B	15″
21/22. IX .85	1.occ.3	3	3	50 cm	V	10″
24/25. IX .85	3.ecl.4	3	3	50 cm	V	10″
25/26. IX .85	3.ecl.1	3	3	50 cm	V	10″
08/09. X .85	1.ecl.2	2	2	50 cm	V	15″
22/23. X .85	1.occ.2	1	0	50 cm	V	10″
	1.ecl.2	1	–	50 cm	V	10″
27/28. X .85	2.ecl.1	3	3	50 cm	B	10″
14/15. X .85	3.ecl.1	1	2	1 m	V	15″
21/22. X .85	3.occ.1	3	2	50 cm	B	10″
	3.ecl.1	2	–	50 cm	B	10″
08/09. IV .86	2.occ.1	3	0	50 cm	V	15″

Notes: (a): 3 = No problem; 2 = Technical problem; 1 = Bad weather
(b): 3 = Strong phenomenon; 2 = Visible; 1 = Faint; 0 = Not visible

infrared for Neptunian and Uranian occultations leading to the discovery and study of rings around these planets, as well as in the visible to search for flares and outbursts.

As the acquisition is made in pulse-counting mode, it is of course possible to gather or smooth the data afterwards, in order to obtain any time resolution higher than 50 ms.

In the case of the mutual phenomena, it soon turned out that the number of interruptions in the acquisition which were necessary to recentre the satellites in the diaphragm was a serious handicap. We therefore introduced a splitting mirror in the large field eye-piece. In this way, it was possible to guide the telescope during the phenomena without interruption.

Two types of photomultipliers have been used: either the EMI 6256 (S-13), or the QUANTACON RCA-31034 (Ga-As). Both are equally good for this purpose. So, the selection was simply based on the following observers needs, in order to avoid too many instrument changes. The filters used were the Johnson V with the EMI photomultiplier and B with the QUANTACON (the satellites of Jupiter are too bright to be observed in V with this photomultiplier without damaging the tube).

The diaphragm employed depended on the weather and was to some extent determined by the type of the phenomenon observed (for an eclipse, the smallest diaphragm is the best one, as you need to follow only one satellite).

3. The Results

Table 1 gives a summary of our observations. Figure 1 shows a group of observations made of an event. Some phenomena have been observed very clearly (Figs. 2, 3, 4) while some others were not seen. A preliminary analysis appears to show good agreement between theory and observations for the timing of the phenomena.

Mutual phenomena do not always occur at the most convenient time, and we have often had to deal with difficult observing conditions, either during twilight when the sky brightness changed rapidly, or at very high airmass. On such occasions, the events could sometimes be hardly observable. While some observations were lost for meteorological reasons, none were lost due to technical problems.

Finally, we note that the major challenge when analyzing the data will be to measure the duration of a phenomenon. Figures 5 and 6 represent the same observation, but the data have been binned to different time resolutions, 400 ms and 800 ms respectively. Using the same graphic method, however, we find that the two data representations give a difference of 26 seconds in duration (corresponding to 8%). The timing of the minimum agrees within .8 second. We thus note that the determination of the intensity and maximum of a phenomenon is far more accurate than an estimate of its duration. Our observations should point out to observers using a conventional photometer how difficult it is to determine the beginning and end of such an event.

4. Conclusion

We could observe a large amount of mutual phenomena at La Silla, even though generally the July–September period is not especially good for photometric observations. The ESO contribution to the campaign is therefore quite substantial.

A workshop organized by the Bureau des Longitudes took place this April, in Bagnères-de-Bigorre (Pic-du-Midi Observatory) to discuss the first results of the PHEMU 85 campaign. Observations carried out in many places in France, Brasil, Spain and Italy were presented. Table 2 shows a summary of all observations made during this campaign. Theoreticians working in celestial mechanics will now have to interpret them, and start their computations to improve the present models. We should

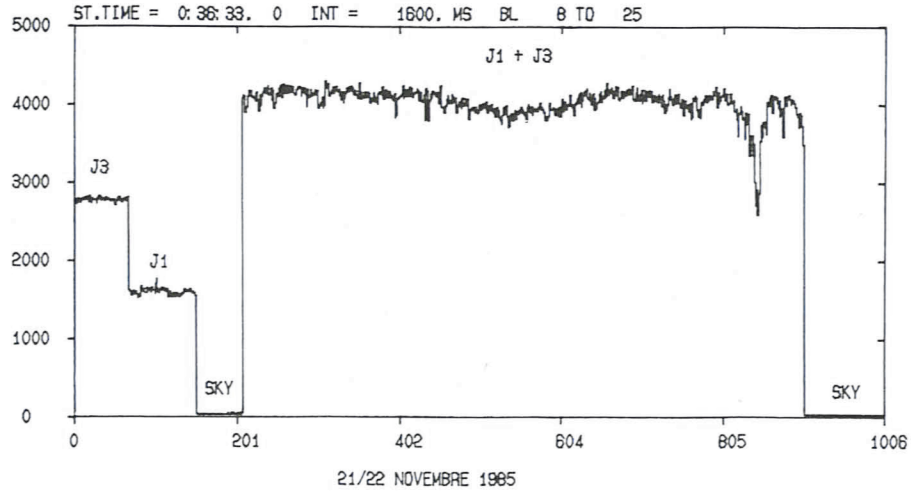

Figure 1: *Sequence of observations made for the occultation of IO (J1) by GANYMEDE (J3), on November 21, 1985, showing the relative intensities of each satellite, of the sky, and of the phenomenon. ST. TIME is the starting UT time, and one time unit is 1,600 ms. Blocks 8 to 25 were added on this picture.*

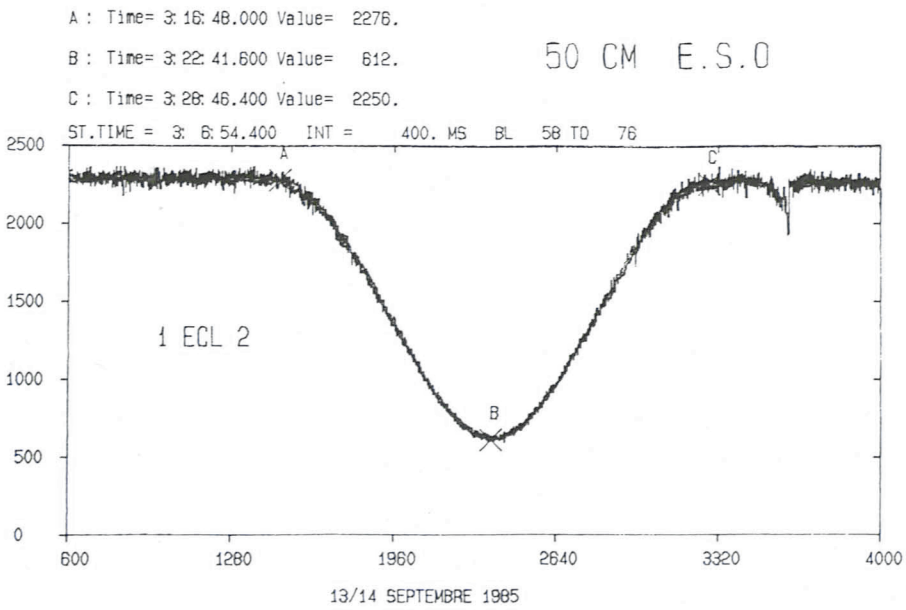

Figure 2: *IO (J1) eclipses EUROPA (J2) on September 13, 1985. The time unit on this picture is 400 ms, and 18 blocks have been added. The points A, B, C have been determined graphically through the reduction programme available at La Silla.*

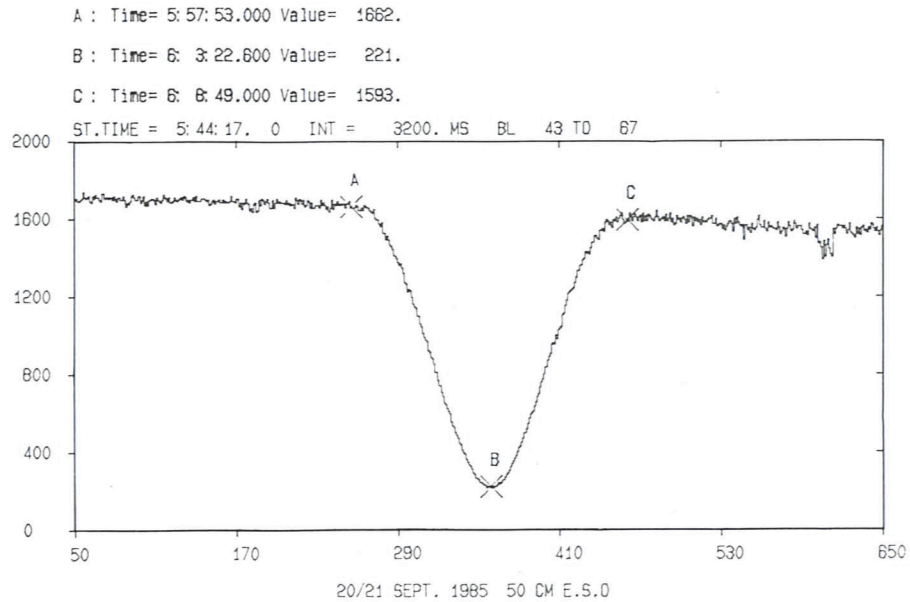

Figure 3: *IO occults EUROPA on September 20, 1985.*

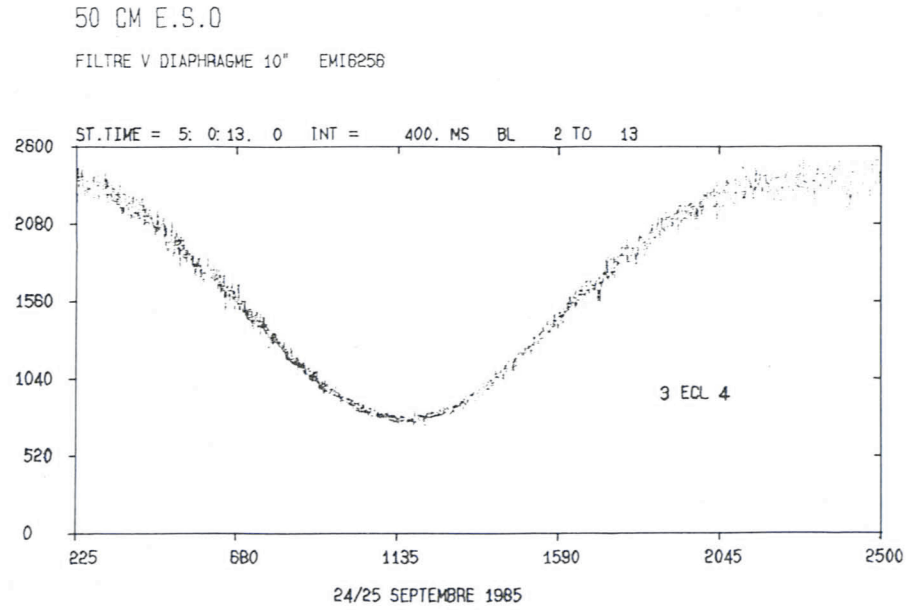

Figure 4: *CALLISTO (J4) is eclipsed by GANYMEDE (J3) on September 24, 1985.*

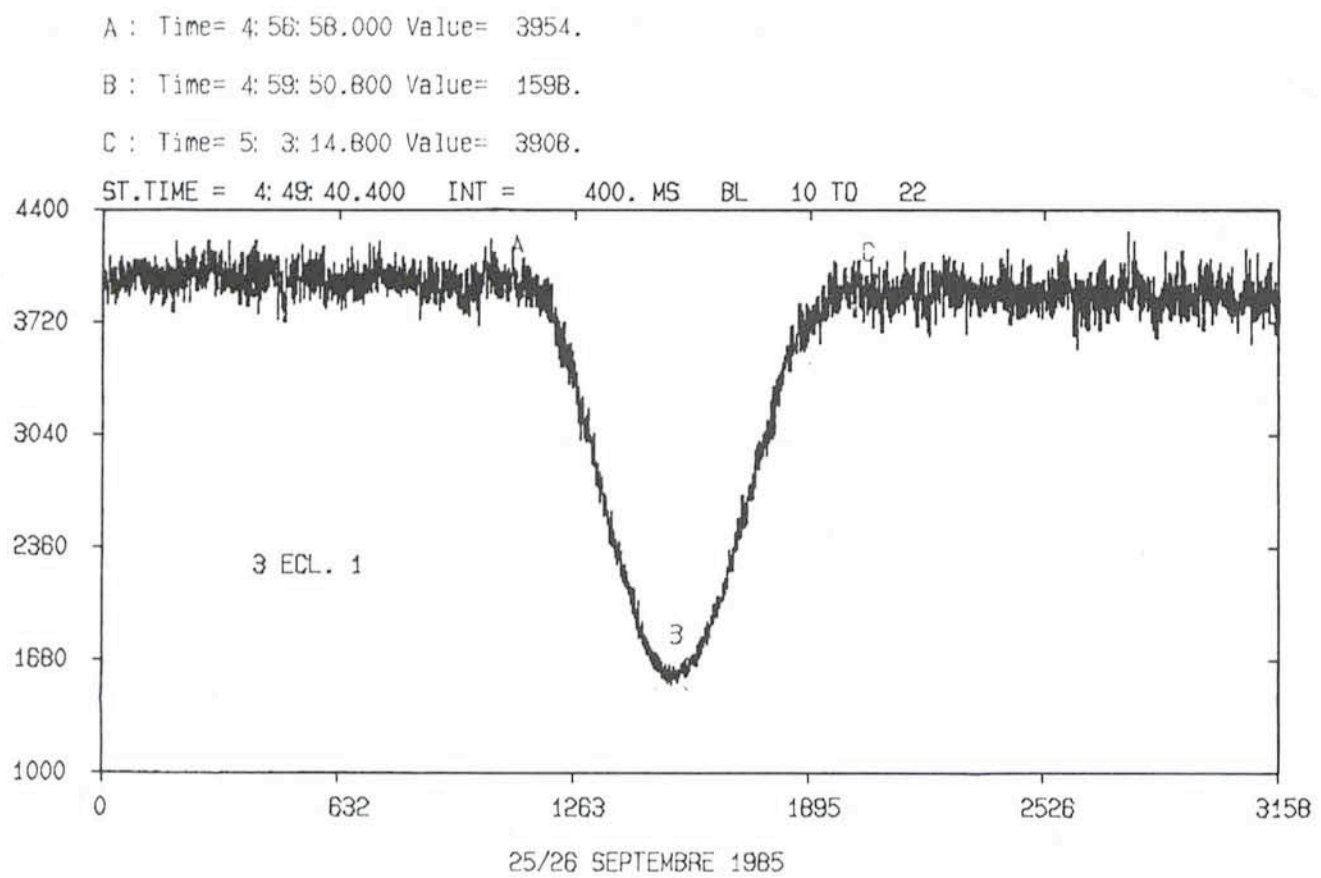

Figure 5: *GANYMEDE eclipses IO on September 25, 1985. The time resolution has been set to 400 ms, and the graphic determination gives a phenomenon duration of 6 mn 17 s.*

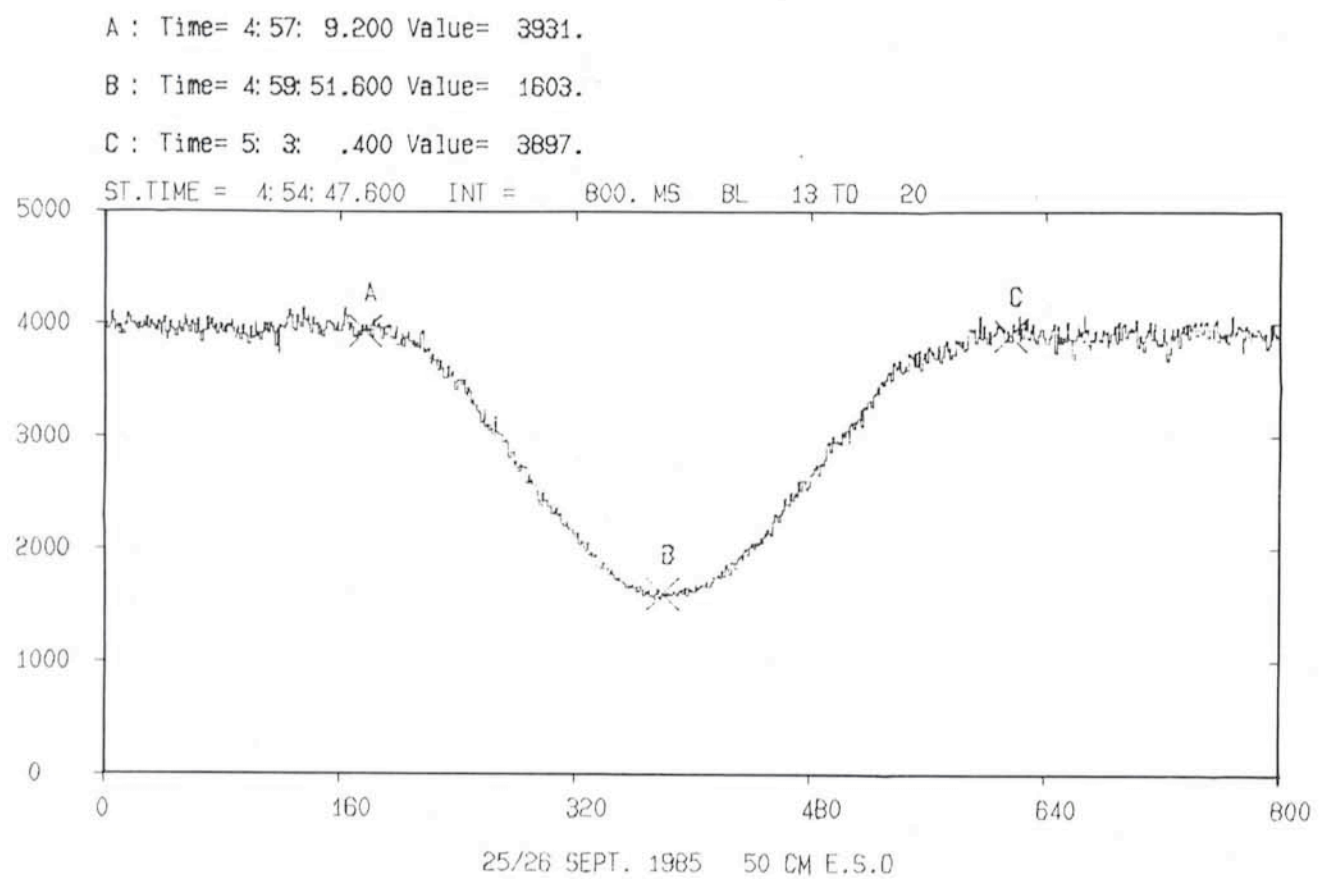

Figure 6: *Same observation as for Figure 5 but now the data are binned with a time resolution of 800 ms. The same graphics method gives a duration of 5 mn 51 s.*

TABLE 2

Observ.	Number of light-curves obtained (a)				Number of good non visual light-curves	Number of events	
						observable	observed
	PP	VD	PH	VI			
OHP	23	–	–	–	15		
CHIRAN	7	–	–	–	3		
OPMT	–	21	–	–	18		
NICE	19	4	–	–	10		
CERGA	7	–	–	–	6		
MEUDON	6	23	–	–	15		
PARIS	10	–	–	–	8	74	52
BORDEAUX	7	–	–	–	4		
TERAMO	19	–	–	–	16		
CATANIA	11	–	–	–	7		
GEOS	1	–	–	81	1		
GEA, Barcelona	10	–	–	9	9		
Miscel.	–	7	5	20	?		
ESO, CHILE	25	–	–	–	23	31	30
LNA, BRAZIL	9	–	–	–	8		
SUMS	154	55	5	90	143	105	82
	209		95				
	304						

Notes: (a): PP = Photoelectrical photometry; VD = Video recording; PH = Photographic photometry; VI = Visual photometry

stress that it is the first time that such a campaign gives so many results and we can already see that although another one will certainly be necessary (in 12 years!), it might well be the last one, provided that the next harvest is as rich as the '85 one.

Acknowledgements

Our best thanks go to F. Gutierrez for his continuous help in managing the software during these observations, and to M. Maugis for his support in the electronics.

List of ESO Preprints

June – August 1986

445. B. Reipurth and G. Gee: Star Formation in Bok Globules and Low-Mass Clouds. III. Barnard 62. *Astronomy and Astrophysics.* June 1986.
446. A. Tornambè and F. Matteucci: Type I SNe from Double Degenerate CO Dwarfs and their Rate in the Solar Neighbourhood. *Monthly Notices of the Royal Astronomical Society.* June 1986.
447. P. Crane, D.J. Hegyi, N. Mandolesi and A.C. Danks: Cosmic Background Radiation Temperature from CN Absorption. *Astrophysical Journal.* June 1986.
448. F. Murtagh: Clustering Techniques and their Applications. *Data Analysis and Astronomy,* Plenum Press. June 1986.
449. A. Terzan, Ch. Turati and Ch. Ounnas: A Photometric Study of the Bright Cloud B in Sagittarius: V. 185 New Proper Motion Stars. *Astronomy and Astrophysics.* June 1986.
450. E. Giraud: A Tully-Fisher Relation for Central Magnitudes of Galaxies in the B, V System. *Astronomy and Astrophysics.* July 1986.
451. G. Contopoulos, H. Varvoglis and B. Barbanis: Large Degree Stochasticity in a Galactic Model. *Astronomy and Astrophysics.* July 1986.
452. E.I. Robson et al.: The Rise and Fall of the Quasar 3C273. *Nature.* July 1986.
453. E. Hummel et al.: The Central Region of NGC 613. Evidence for an Accelerated Collimated Outflow. *Astronomy and Astrophysics.* July 1986.
454. A. Llebaria, J.-L. Nieto and S. di Serego Alighieri: On the Non-Linearity of the ESA Photon Counting Detector. *Astronomy and Astrophysics.* July 1986.
455. M.W. Pakull and L.P. Angebault: Detection of an X-Ray Ionized Nebula Around the Black Hole Candidate Binary LMC X-1. *Nature.* July 1986.
456. T.J.-L. Courvoisier, J. Bell-Burnell and A. Blécha: Optical and Infrared Study of the Three Quasars OX 169, NRAO 140 and 3C446. *Astronomy and Astrophysics.* August 1986.
457. F. Matteucci: The Evolution of CNO Abundances in Galaxies. *P.A.S.P.* August 1986.
458. R. Gathier: Radio Observations of Young Planetary Nebulae. *The Late Stages of Stellar Evolution.* Reidel, Dordrecht. August 1986.
459. R.H. Sanders: Alternatives to Dark Matter. *Monthly Notices of the Royal Astronomical Society.* August 1986.
460. C. Barbieri et al.: Quasar Candidates in the Field of SA 94 – II. Objective-Prism Classification of the US Objects. *Astronomy and Astrophysics.* August 1986.
461. L. Binette and A. Robinson: Fossil Nebulae in the Context of Active Galaxies. I. Time Evolution of a Single Cloud. *Astronomy and Astrophysics.* August 1986.
462. D. Baade: Ground-Based Observations of Intrinsic Variations in O, Of and Wolf-Rayet Stars. *NASA/CNRS Monograph Series on Nonthermal Phenomena in Stellar Atmospheres,* volume *O, Of and Wolf-Rayet Stars,* eds. P.S. Conti and A.B. Underhill. August 1986.
463. B.E.J. Pagel: Helium, Nitrogen and Oxygen Abundances in Blue Compact Galaxies and the Primordial Helium Abundance. Paper delivered to the Paris (IAP) Conference on Nucleosynthesis, 1986, July 7–11. August 1986.
464. J.M. Rodriguez Espinosa et al.: Star Formation in Seyfert Galaxies. *Astrophysical Journal.* August 1986.

VLT REPORTS

In connection with ESO's planned Very Large Telescope the following VLT Reports have recently been published:

No. 41: A First Evaluation of the Effects of Wind Loading on the Concept of the ESO Very Large Telescope. By L. Zago. June 1985.

No. 42: Aperture Synthesis (Spatial Interferometry) with the Very Large Telescope. An Interim Report by the ESO/VLT Working Group on Interferometry. October 1985.

No. 43: Site Testing at Cerro Paranal – Results from 1983. By A. Ardeberg, H. Lindgren and I. Lundström. December 1985.

No. 44: Very Large Telescope. An Interim Report by the ESO Study Group. January 1986.

No. 45: Site Testing at Cerro Paranal – Results from 1984. By A. Ardeberg, H. Lindgren and I. Lundström. March 1986.

No. 46: Enclosure and Buildings for the ESO Very Large Telescope. By L. Zago. May 1986.

No. 47: Adaptive Optics for ESO's Very Large Telescope (VLT) Project. By F. Merkle. May 1986.

No. 48: Comparison of Meteorological Conditions on Chilean Sites. Annual Summary 1985. By M. Sarazin. June 1986.

No. 49: Interferometric Imaging with the Very Large Telescope. Final Report. By the ESO/VLT Working Group on Interferometry. June 1986.

No. 50: VLT Working Group on High Resolution Spectroscopy. Final Report. June 1986.

No. 51: VLT Working Group on Infrared Aspects. Final Report. July 1986.

No. 52: Report to the ESO VLT Projekt of the Working Group on Imaging and Low Resolution Spectroscopy. July 1986.

VLT Reports No. 1–40 were mainly for internal purposes and are meanwhile out of print.

The Unusual Barred S0 Galaxy NGC 4546

G. GALLETTA, Institute of Astronomy, University of Padua, Italy

Introduction

At the beginning of May 1986, during an observing run concerning the stellar kinematics in barred S0 galaxies, we observed the SB0 NGC 4546, an almost edge-on disk system, finding the presence of a very peculiar phenomenon: within the galaxy, the gas clouds are moving with similar velocities but in opposite direction with respect to the stars. This fact, present also at different position angles, makes this galaxy a unique case of disk system with large-scale, retrograde gaseous motions with respect to the stars.

The observations of NGC 4546 are part of a larger programme of study for the structure and the kinematics of SB0's, programme started at ESO in 1984 and including at the present time spectroscopic and photometric data for four galaxies. The goals of this programme are to reach a good knowledge of the kinematical properties of disk galaxies in the presence of a bar and an appropriate analysis of the stellar orbits within the bars, considered as typical triaxial structures. As a first result, we found the existence of some peculiarities in the velocity field of the first SB0 studied, NGC 6684: an oval distortion of the stellar disk and the presence of elongated stellar orbits within the bar. They confirm the existence of an oval distortion suggested by the study of some barred disk galaxies (Kormendy, 1979, 1983) and invoked also to explain and stabilize the structure of "spindle" galaxies, a type of S0's with a luminous and extended gas disk perpendicular to its symmetry plane (Schweizer, 1983).

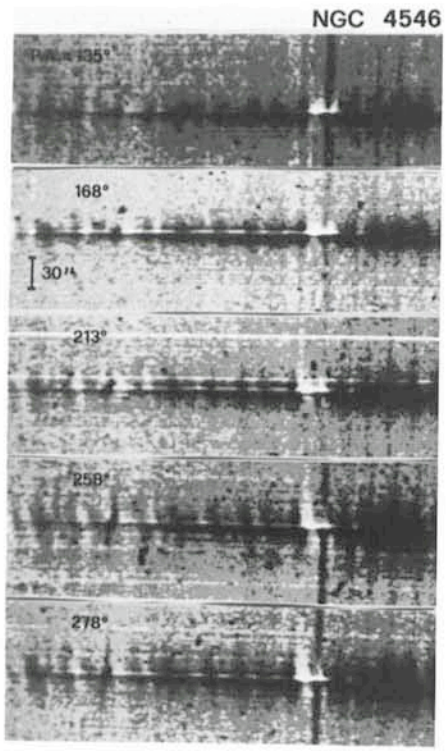

Figure 1: *Composition of the spectra of NGC 4546 at six different position angles. To make the lines more evident, the continuum has been partially subtracted in all the images. The emission lines are represented by [OIII] features (left of the spectra), with only λ 5007 clearly visible. The intense absorption lines visible in the portion of the spectra shown here are Mg I λ 5175.4, near the 5200.0 [NI] sky lines, and Ca+Fe λ 5269.0. Note that nearer to the major axis (P.A. = 258°), the emission and the absorption lines tend to be inclined because of the rotation in opposite directions. This fact characterizes the exceptionality of the kinematics of this stellar system.*

The selection of NGC 4546 as a candidate for spectroscopic and photometric studies derives from several characteristics: (i) it is quite a luminous galaxy, with B magnitude 11.3; (ii) its ellipticity is 0.52, indicating an almost edge-on system where it is possible to study the bar along one of its principal planes ; (iii) it shows the presence of the [OII] lines at λλ 3727–29 Å (Humason et al. 1956); (iv) it possesses an HI rotating disk with a velocity width for the line of 350 km/s (Bieging, 1978). All these properties make this galaxy an interesting subject of study.

Observations and Data Analysis

NGC 4546 has been studied in the nights of May 4 and 5, 1986, with the CCD and the Boller and Chivens spectrograph of the 2.2-m ESO-MPI telescope at six different position angles. The exposure times were ranging from 90^m for minor axis and intermediate angles spectra to 120^m for the major axis spectrum, at P.A. = 258° (Figure 1). The dispersion used was 1.77 Å/pixel (grating 10, second order) while the scale perpendicular to the dispersion was 1.808 arcsec pix^{-1} or about 59 arcsec mm^{-1}. The spectral interval explored was ranging from 4900 to 5700 Å. In order to study the extension of the gas and its motions outside the main galactic plane, two 60^m spectra were secured offsetting the centre of the slit by 5" on both sides of the nucleus (NW and SE, Figure 2) and perpendicularly to the major axis. An additional major axis spectrum of 15^m exposure was kindly taken for us with the same instrument by S. di Serego Alighieri on the night of May 6 at lower dispersion (5.16 Å pixel^{-1}, grating 16) in the interval λλ 4730–7300 Å.

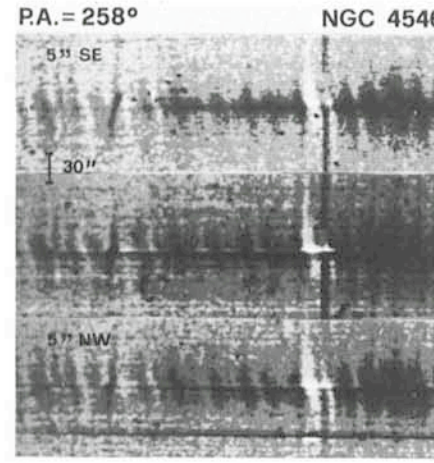

Figure 2: *The same as Figure 1, but for the spectrum of the major axis (centre) and two offset spectra at the same P.A. but at 5" (430 pc) SE and NW from the nucleus. The extension of the phenomenon of counter rotation between stars and gas appears with similar behaviour.*

In addition to these spectroscopic data, V, Hα and Gunn I frames were recorded with the CCD of the 1.5-m Danish telescope on the nights of May 6 and 7, 1986. The image of the galaxy is shown in Figure 3, from a 1^m (top) and a 15^m (bottom) V exposure. From these images, it appears that the galaxy shows a disk strongly inclined to the plane of the sky, as stated by the presence in the shorter exposure of Figure 3 of two spindles in the outer isophotes. The bar, whose presence has been mentioned by de Vaucouleurs et al. (1976), appears just like an irregularity of the isophotes roughly at 45° NE of the major axis and is completely embedded in the galaxy body. A faint absorption, probably a dust lane, appears at P.A. = 248°, ten degrees SW of the major axis. In agreement with its relative closeness, 17.8 Mpc according to the group distance (Virgo V, de Vaucouleurs, 1975), in the deeper exposure, NGC 4546 reveals in its halo the presence of a number of faint, almost stellar images, probably globular clusters. Some of them are visible in Figure 3 (bottom).

In the spectra of Figure 1, to make the lines more evident, the continuum has been partially subtracted in all the images, showing the complex texture of the spectral lines. The [OIII] emission lines are visible, but the faintest one, λ 4959, is too faint to give a measurable signal, also because of the many ab-

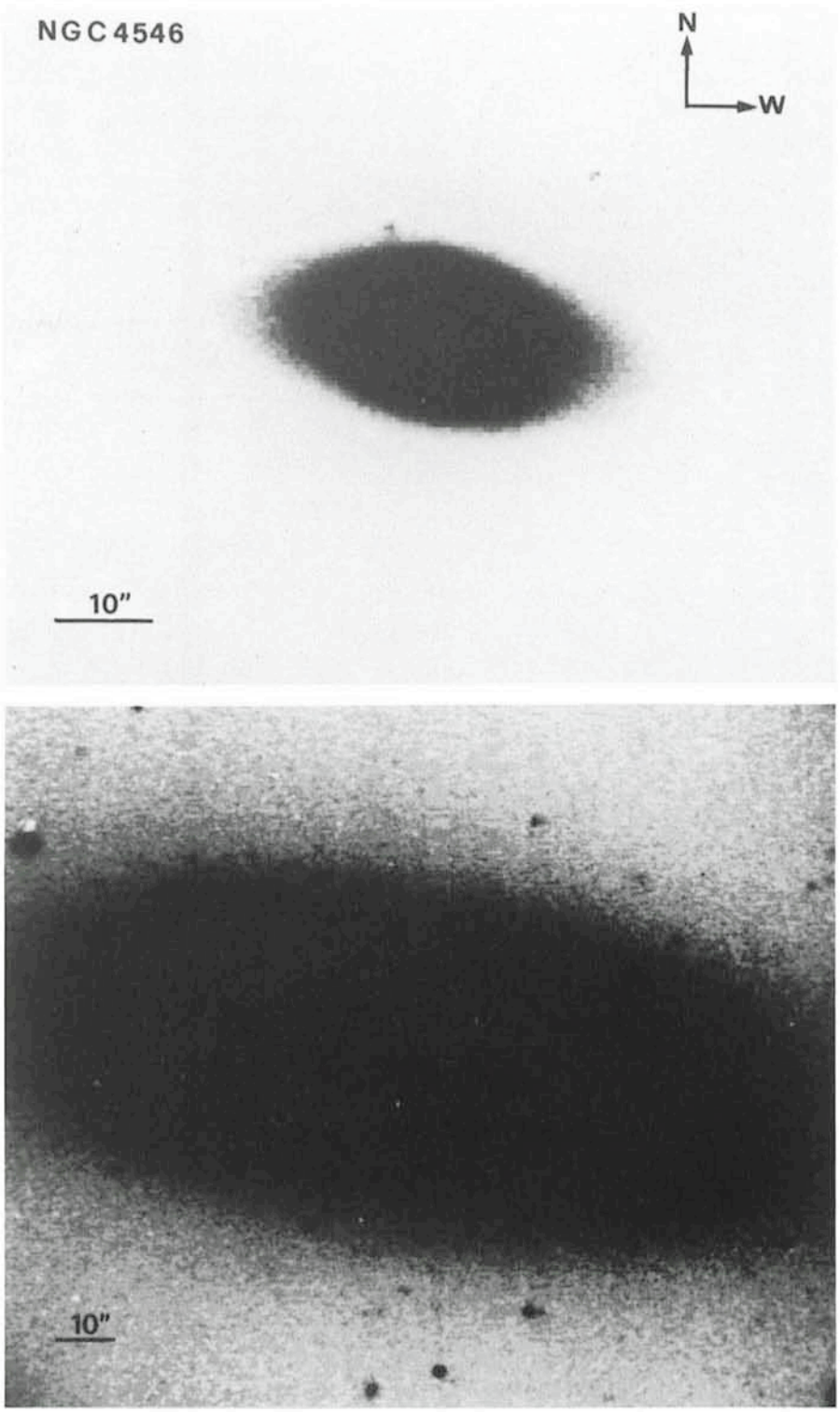

Figure 3: *Two images of the galaxy, from a 1^m (top) and a 15^m (bottom) V exposure. The bar appears just like an irregularity of the isophotes roughly at 45° NE of the major axis and is completely embedded in the galaxy body. A faint absorption, probably a dust lane, is visible ten degrees SW of the major axis. In the deeper exposure, NGC 4546 reveals in its halo the presence of a number of faint, almost stellar images, probably globular clusters.*

sorption features that are intersecting it with opposite inclination. The spectral features of MG I λ 5175.4, near the 5200.0 [NI] sky lines, Ca+Fe λ 5269.0 and Fe λ 5331.5 are visible in absorption and are the predominant lines in the spectra. From the low dispersion spectrum it is possible to see also the presence of the emission lines Hα, [NII] λλ 6548–84 and [SII] λλ 6717–31.

All the spectra were preliminarily reduced with the IHAP package at the Padova HP computer centre and analysed kinematically by interpolating Gaussian functions to the more intense emission and absorption lines. No attempt has been made to add together scan lines, in order to increase the signal-to-noise ratio. This process was repeated for each spectrum and for each scan line using a batch IHAP procedure. A sample of the results is shown in Figures 4 and 5, where the rotation curves measured from emission and absorption lines along the major axis of the galaxy are plotted. A more complete reduction of the velocity field will be performed during the next months using the technique of the Fourier Quotient which produces also the velocity dispersion of the stars.

Discussion

In most of the spectra (Figure 1), the gas lines appear inclined because of the rotation in a direction opposite to that of the stellar lines, indicating opposite directions of motion. This fact characterizes the exceptionality of the kinematics of this stellar system. In fact, at the present time, no S0 or spiral galaxy is known to possess this characteristic. The same behaviour is present in the spectra taken parallel to the major axis but with a ± 5″ offset with respect to the nucleus (Figure 2). At the assumed distance of 17.8 Mpc, these offsets correspond to about ± 430 pc, showing that the phenomenon is quite extended.

A look at Figure 1 shows that along the minor axis (P.A. = 168°) the stars exhibit almost no rotation, as indicated by the lack of inclination of the absorption lines. At the same position angle, on the contrary, the gas presents residual motions that decrease until, at 135°, about along the minor axis of the bar, the emission lines tend to straighten. This fact indicates that the lines of nodes of the planes where the gas and the stars are moving are not at the same position angle. This kinematical difference is confirmed by the analysis of the velocity gradients. Their values for the stellar motions show a cosine decrease with the P.A. reaching a maximum of about 12 km s^{-1} arcsec^{-1} at P.A. = 80°, very close to the major axis of the galaxy, in agreement with the expectation for circular orbits on the galactic plane. Peculiar orbits appear in the inner part of the system. The study of the gas rises more complex problems: in fact, along the major axis, when the slit crosses the bar, a dip of the rotation curves towards lower velocity is visible. This characteristic disappears in the offset spectrum at 5″ SE, indicating gas flow or elongated orbits within the bar. The same behaviour is presented by the analysis of the velocity gradients of emission lines, which follow an approximate cosine law with line of the nodes at 225° (near the bar major axis) and a

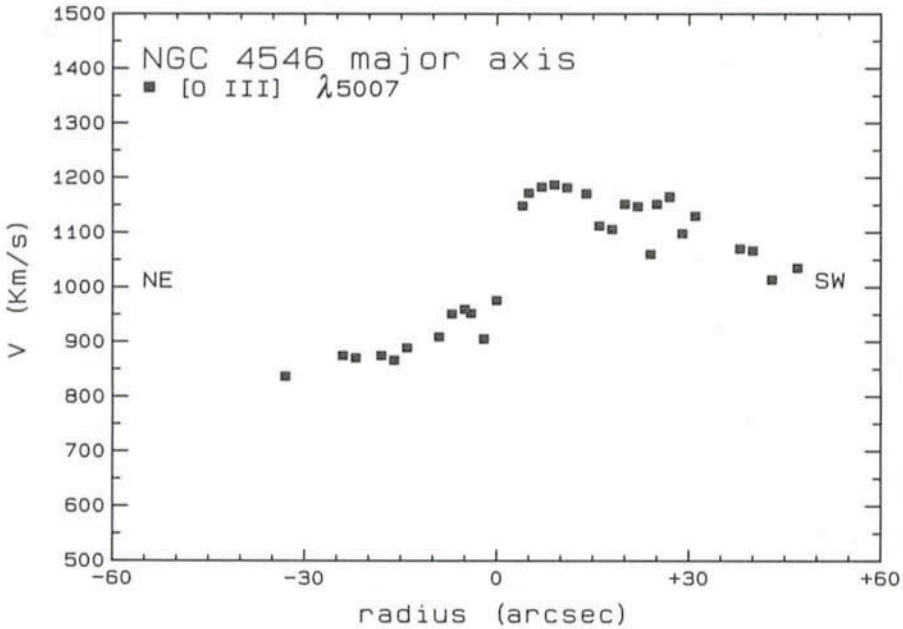

Figure 4: *Rotation curve for the gas along the major axis, from a Gaussian interpolation of the spectral line [OIII] λ 5007.*

maximum of 12.5 km s^{-1} $arcsec^{-1}$ gradient, with the exception of the rotation curve measured at P.A. = 213°, whose inner slope of about 5 km s^{-1} $arcsec^{-1}$ is well down the expected value off 15 km s^{-1} $arcsec^{-1}$.

Then, if all these motions are evolving along a plane, the plane of the gas is not coplanar with that of the stars and the gas existing within the galaxy shows a radial flow along the bar which could explain the asymmetries observed. In addition, since the maximum extension of the gas is observed near the major axis, about 30° from its direction of maximum velocity gradient, the gas itself appears confined within a more or less asymmetric disk, of projected dimension 1.7 × 8.2 kpc, not aligned with the stellar disk of the galaxy neither with the bar.

Where did this gas come from? One possible hypothesis is that the gas is circulating in one of the retrograde families of orbits possible in triaxial systems (de Zeeuw and Merrit 1983) or the bars (Freeman 1966, Contopoulos and Papayannopoulos 1980). It is expected in this case that, since the gas clouds are moving together with the stars in a narrow tube, this prevents their collapse by collision or dynamical friction. But this phenomenon involves confined regions of space, contrary to that observed. The same problem is present for a second possibility: that we are observing gas confined in a retrograde portion of a "hot" velocity field, similar to that found for some globular clusters in our galactic halo (Oort 1965). With the exception of the two above-mentioned cases, we find it difficult to imagine a mechanism that discriminates between gas and stars with common origin, driving it in two opposite directions of rotation. A third and alternative hypothesis is that the gas has not the same origin as the stars but is the result of a more or less recent acquisition, and comes from a retrograde collision with a dust cloud or a gas-rich dwarf galaxy. The discovery of hot stars or HI bridges with other close stellar systems would give an interesting check of this hypothesis.

Concluding this short note, we would like to draw the attention to another case of counter-rotation known in the literature, although the nature of this system is quite different from the disk galaxy considered here: along the major axis of the galaxy NGC 7097, classified E4, Caldwell et al. (1986) have measured a gas rotation of 200 km/s superimposed on a slow stellar rotation of a few tens of km/s in opposite direction.

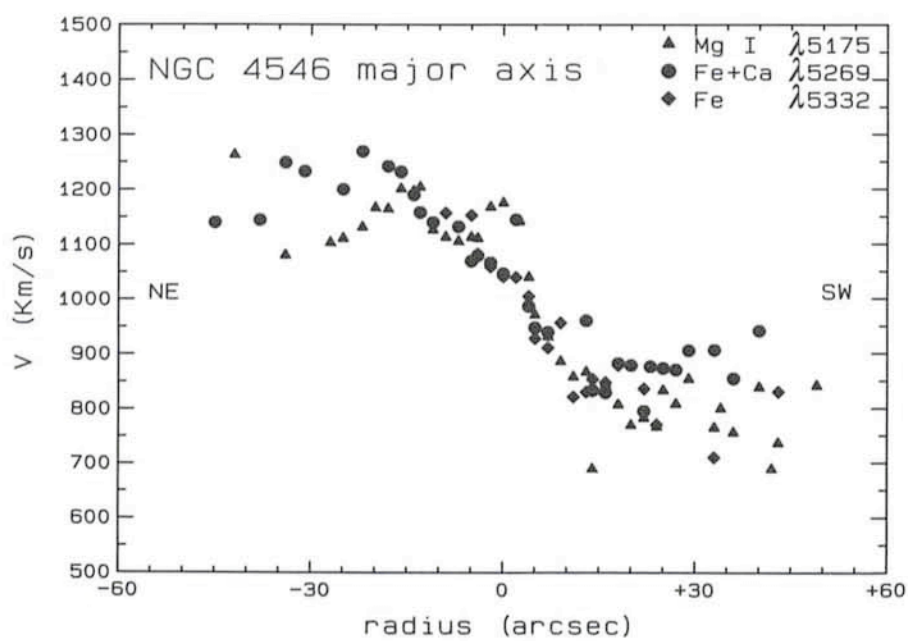

Figure 5: *The same as Figure 4, but for the stars. The stellar lines used are labelled with different symbols.*

Applications for Observing Time at La Silla

Period 39 (April 1–October 1, 1987)

Please do not forget that your proposals should reach the Section Visiting Astronomers **before October 15, 1986.**

References

Bieging, J.H., 1978, *Astron. and Astrophys.* **64,** 26.

Caldwell, N., Kirshner, R.P., Richstone, D., 1986, *Astrophys. J.,* **305,** 136.

Contopoulos, G. and Papayannopoulos, Th., 1980, Astron. and Astrophys., **92,** 33.

de Vaucouleurs, G., 1975, in *Stars and Stellar Systems,* The University of Chicago Press, Vol. **IX,** p. 584.

de Vaucouleurs, G., de Vaucouleurs, A. and Corwin, H.G.Jr. 1976, RC2, *Second Reference Cat. of bright galaxies,* Austin, Univers. of Texas Press.

de Zeeuw, T. and Merrit, D., 1983, *Astrophys. J.,* **267,** 571.

Freeman, K.C., 1966, *Mon. Not. of Royal Astr. Soc.,* **134,** 1.

Humason, M.L., Mayall, N.V. and Sandage, A.R., 1956, *Astron.J.* **61,** 101.

Kormendy, J., 1979, *Astrophys.J.,* **227,** 714.

Kormendy, J., 1983, *Astrophys.J.,* **275,** 529.

Oort, J.H., 1965, in *Stars and Stellar Systems,* The University of Chicago Press, Vol. **V,** p. 486.

Schweizer, F., 1983, IAU Symp. no. **100,** p. 319.

Radio to X-Ray Observations of the Quasar 3C 273

T.J.-L. COURVOISIER[1], The Space Telescope European Coordinating Facility, European Southern Observatory

Quasars and active galactic nuclei are the most luminous objects we know. Their emission is distributed over all the spectral bands from radio waves to gamma rays, in such a way that we measure approximately the same flux in each frequency decade of the electromagnetic spectrum. Furthermore, large continuum flux variations are known to occur in most of the spectral bands. The very high luminosity (up to 10^{14} $L_\odot$) and the very small size (≈ 1 light month, as deduced from typical variability time scales) of these objects indicate extreme physical conditions, which we are still far from understanding. The relationships between the variations in the different domains of the spectrum can however provide a powerful tool to study the interplay of the various emission components and therefore to understand the physical relations between the different cooling processes and associated electron populations.

In order to study these relations and also to measure the overall continuum emission spectrum avoiding the uncertainties due to the large flux variations observed in the different spectral domains, we performed repeated coordinated multi-frequency observations of the bright quasar 3C 273 from radio waves to X-rays.

Repeated observations of the continuum emission over most of the spectrum are only possible for a few active galactic nuclei which are sufficiently bright to obtain precise and absolutely calibrated flux measurements in relatively short exposures from ground-based telescopes and by space-born instrumentation. The bright and intrinsically luminous quasar 3C 273 was selected for a series of observations during the lifetime of the European X-ray satellite EXOSAT. During more than 2 years, starting in December 1983, we observed 3C 273 in the X-rays with EXOSAT, in the ultraviolet light with the satellite IUE, optically using the instrumentation of ESO and the Swiss telescope at La Silla, in the infrared domain with the UK infrared telescope in Hawaii and at ESO, in the mm band also at the UK infrared telescope and in the radio waves mostly with the Metsaehovi radio telescope in Finland. The results of this effort will be published shortly (1), a presentation of the first data obtained was given in the *Messenger* in 1984 (ref. 2).

Several observations of 3C 273 in each of the spectral domains radio, mm, infrared, optical, ultraviolet, X-rays were performed each observing season (December–July). They showed that there are at least 4 distinct cooling processes which dominate the continuum emission in the far infrared, near infrared, optical-ultraviolet and X-ray domains respectively. That the information acquired in the different bands is not redundant is shown by the fact that flux variations are not correlated in any simple way in the different spectral domains.

Our observations revealed that the flux observed in the different spectral domains varied with time in a complex and seemingly uncorrelated way: We observed an irregular decrease by a factor ≈ 2 in the hard X-rays (2–10 keV, observed in EXOSAT's Medium Energy detectors) between December 1983 and May 1984. The fastest flux variation during this period implies a change by a factor 2 in ≈ 30 days in this spectral region. At the same epoch the soft X-rays (≈ 0.7 keV, observed in EXOSAT's Low Energy telescope) decreased by about 30%, no comparable change was observed in any of the other bands. The long term behaviour of 3C 273 between 1984 and 1986 is characterized by a ≈ 20% increase in the ultraviolet flux, a nearly constant flux in the optical and near infrared bands (J, H, K, L), with the possible exception of a "dip" by a factor ≈ 2 lasting one month in the near infrared, and a decrease at longer wavelengths by a factor ≈ 2 in the 10 μm and 20 μm region, a factor ≈ 4 in the mm region and a factor ≈ 2 in the radio waves. The soft X-ray flux varied between all observations by 20–30% with no obvious trend, and the hard X-ray flux remained nearly constant after its initial large decrease until 1985 to increase again by ≈ 30% at the beginning of 1986. The loss of EXOSAT in the spring of 1986 did not allow the monitoring of this new event.

The continuum spectrum shape as we observed it at the beginning of 1984 is shown in Figure 1. It can be described mathematically by the sum of the following functions: one power law of slope (energy index) ≈ 0.6 extending from the radio domain to ≈ 10 microns, another power law of slope ≈ 1.7 in the near infrared region, 2 black body distributions of T $\approx$ 20000 K and $\approx$ 120000 K and a power law with a slope of ≈ 0.45 describing the X-ray emission. The parameters describing the spectrum were determined by fitting the total function to the observed continuum data. The large gap in the observed spectrum extending from the ultraviolet (as observed by IUE) and the soft X-rays (observed by the Low Energy telescope of EXOSAT) makes it difficult to describe the exact

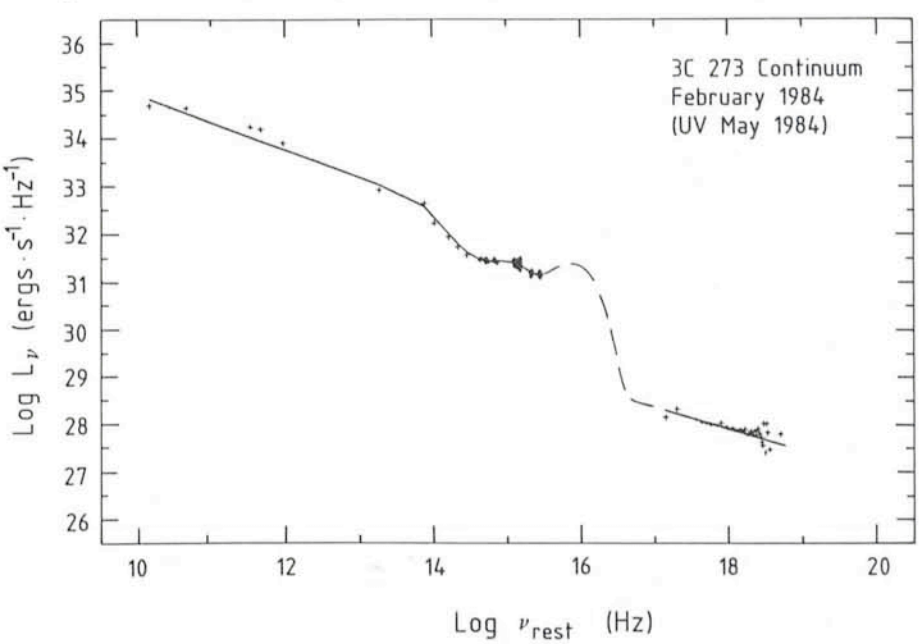

Figure 1: *February 1984 (UV in May) continuum energy distribution of the Quasar 3C 273 from the radio wave ($\approx 10^{10}$ Hz) to the X-ray ($\approx 10^{18}$ Hz) domains. The data are given as crosses and the fitted function (see the text) as a continuous line. The best fit parameters imply a large far ultraviolet "bump" (interrupted line), which will need confirmation with future instrumentation.*

[1] Affiliated to the Astrophysics Division, Space Science Department, ESA.

shape of the extreme ultraviolet bump which is implied by the available data. This is all the more regrettable since the largest contributions to the total luminosity could come from this bump at least at certain epochs. (At other epochs, the luminosity is probably dominated by the hard X-ray emission, up to a few 100's keV).

The flux variations observed in the different bands imply changes in the spectral parameters. The January 1986 spectrum is thus significantly flatter in the far infrared-mm (down to $\approx 5-10$ μm) domain than the 1984 spectrum, whereas the near infrared emission (between ≈ 1 μm and ≈ 5 μm) remained very stable (3). The slope of the X-ray emission remained, however, nearly constant when the flux changed.

The data we have collected can be used to test theoretical model predictions; they are, however, still far too scarce to constrain the models sufficiently to provide a univocal description of the quasar phenomenon. The complex pattern of time variations also provided evidence for a new spectral component: The different (and unexpected) behaviour observed in the mm-infrared domain above $\approx 5-10$ μm and below this limit (3) showed that the near infrared emission cannot be dominated by the high energy tail of the far infrared component, which is generally thought to be of synchrotron origin. The near infrared emission must therefore have an origin of its own, which we do not understand yet. Another example of different time variability patterns is found in the mm-infrared and the X-ray domains: No large mm-infrared flux variations were observed at the beginning of the campaign while the X-ray flux decreased by a factor ≈ 2. This implies that these two components cannot be emitted by the same electron population, as has often been proposed in the so-called synchrotron self-Compton models.

The time scales of variability in the different bands give useful limits to the size of the respective emission regions provided that no relativistic bulk motion or gross projection effects introduce large correction factors. The sizes we can infer from our observations indicate that the hard X-ray emitting region is of the order of ≈ 1 light month, similar to the near infrared emitting region (provided that the dip we observed is confirmed). The variations seen in the ultraviolet domain prior to our observations (4) also indicate a similar size for the region emitting the (optically thick) blue bump. The variations observed in the far infrared imply a size of less than a few light months. This latter number however cannot be further precised, because of the undersampling of the light curve.

The very different time variation patterns observed in the different bands and the typical variability time scales of ≤ 1 month show the need for numerous more coordinated observations of quasars covering the entire spectrum to reveal the interplay of the different components. Such observing campaigns are difficult to organize as they imply many different observatories around the world and little structure is available to coordinate observations from different institutions. EXOSAT has now finished its life and will not be followed by a European X-ray observing facility for some years. We hope, however, to have access to data from the Japanese X-ray satellite Astro-C to be launched next year to continue our efforts.

References:

1. Courvoisier, T.J.-L., Turner, M., Robson, E.I., Gear, W.K., Staubert, R., Blecha, A., Bouchet, P., Falomo, P., Valtonen, M. and Teräsranta, H., 1986, in preparation.
2. Courvoisier, T.J.-L., 1984, *The Messenger* **37,** September 1984.
3. Robson, E.I., Gear, W.K., Brown, L.M.J., Courvoisier, T.J.-L., Smith, M.G., Griffin, M.J. and Blecha, A., 1986, *Nature,* in press.
4. Courvoisier, T.J.-L. and Ulrich, M.H., 1985, *Nature* **316,** 554.

Modelling Space Telescope Observations

M. ROSA and D. BAADE, The Space Telescope European Coordinating Facility, European Southern Observatory*

1. Introduction

A software package designed to simulate observations obtained with the Hubble Space Telescope (HST) has been developed at the Space Telescope European Coordinating Facility (ST-ECF) at ESO, Garching. This report presents a comprehensive description of the reasoning and scientific, technical and operational background that has led to the development of this HST Model. Examples illustrate how the model is used to predict the actual results of observations.

2. Technical and Scientific Background

2.1. Operational differences between ground-based and HST observing

Observing experience cannot be gathered from handbooks and users guides alone. In the case of ground-based observations, it usually is the result of experiments under real observing conditions.

Often the best instrumental set-up and observational procedure is found only after several trials using mediocre atmospheric conditions to prepare for the really good nights.

In view of the expensive observing time and tight scheduling requirements, such a procedure is prohibitive for Hubble Space Telescope (HST) observations (and also not really desirable for ground-based activities). Furthermore, in the case of HST, almost all programmes will be pushing to the absolute limits of feasibility. In order to assure the utmost scientific return it will not be enough to tune the data reduction software to the limits set by information theory. The observational procedures as well will have to be set up in the most efficient way in order to keep the noise level in the data acquired below the largest tolerable value yet spending the lowest possible amount of the precious observing time allocated.

The optimal use of the HST and its scientific instruments for a given scientific problem will (in general) not be obvious to judge from the technical details of the performance alone. Slight changes in the performance of a given part of an instrument might in fact call for a revision of the entire observational strategy, e.g. the choise of grating and detector combination.

It follows that a system capable of simulating observations with the instruments of HST in advance of the layout of proposals and of the real observations can largely compensate for the lack of experience and of the possibility of interaction in operational procedures.

2.2. Technical differences between dedicated space experiments and HST

Usually astronomical space experiments work in frequency domains inac-

* Affiliated to the Astrophysics Division, Space Science Department, European Space Agency.

cessible from ground and therefore employ telescopes and detectors of highly specialized nature with a very limited range of possible instrumental configurations. Examples are the X- and Gamma-ray experiments and the International Ultraviolet Explorer (IUE), which are free flying laboratory set-ups rather than orbiting versions of ground-based observatories. The IUE for example acquired thousands of exposures in only 4 well-defined, rigidly-fixed spectrographic modes. In such experiments, once the first few raw data are obtained of standard targets, a preliminary instrumental calibration can be produced. This will serve as a means of estimating exposure times and performance for all future exposures to be made of a given type of object.

The (prospective) user of the HST observatory will have to choose between 6 scientific instruments, each of which has a multitude of configurations. Recall that there are two imaging instruments, the Wide-Field and Planetary Camera (WFPC) and the Faint-Object Camera (FOC); two spectrographs, the High-Resolution Spectrograph (HRS) and the Faint-Object Spectrograph (FOS); a High-Speed Photometer (HSP) and the Fine-Guidance Sensor (FGS). The instruments cover the entire wavelength range from 1000 Å to about 1 micron or parts thereof, although with greatly varying efficiencies. The WFPC deploys 8 CCD chips in two focal ratio configurations, 42 filters, 3 polarizers and 3 objective gratings. The FOC consists of 2 intensified photon counting systems imaging at 3 focal ratios with the possibility to insert up to 4 out of 49 different filters, plus one each of 2 polarizers and 5 objective prisms. Spectroscopy with the HRS can be done with two Digicons and 8 gratings with resolutions of 2×10^3, 2×10^4 and 10^5. The FOS also uses two Digicons and offers 6 gratings in medium, 3 gratings or prisms in low resolution mode and spectropolarimetry. HSP consists of 4 image dissector tubes and a photomultiplier, 18 filters, 4 polarimetric filters and an aperture plate with 50 apertures. Finally, the 3 FGS sensors, besides their task of tracking HST during exposures with the other 5 instruments, can perform astrometry in selected wavebands. For more details see the HST Instrument Handbooks and the Call for Proposals distributed by the Space Telescope Science Institute, Baltimore (STScI).

Altogether there are several hundreds of useful modes that can be selected with HST, not including choices to be made for the read-out parameters of the detectors and the freedom in selecting a continuum of central wavelengths for HRS. Simulated HST observations can provide substantial help for the decision among apparently equivalent but slightly different modes to be selected for a given scientific objective. Finally, only the frequently used modes will be covered by the routine calibration process devised for HST operations. It will therefore be most interesting, if not necessary, to obtain a best guess of the performance in the uncalibrated modes through simulations.

2.3. Differences in performance between HST and ground-based telescopes

The detectors and instruments of HST and the observational techniques are generally well known from ground-based observatories. What makes observing with HST so exceptional is its capability to work near the diffraction limit of its 2.5-m mirror since there is no intervening turbulent atmosphere. In addition, the background light, which is already significantly lower because of operation above the earth's atmosphere, is greatly diminished (for point sources) by the gain in spatial resolution of at least a factor of 7 squared, i.e., per area of the PSF the background contamination is suppressed by another factor of 50.

The new side-effects encountered will for instance be the variation of spatial resolution with wavelength (by nearly an order of magnitude over the accessible wavelength range). This will cause variable throughput for the smallest spectrographic and photometric apertures, a variation of image size with effective colour for stars observed through broadband filters, especially in the UV where red leaks are very disturbing, and, finally, a severe undersampling of the point spread function at short wavelengths in some of the cameras. For ground-based observations, these effects are under most circumstances negligible. Further, due to the lack of a sufficient sky signal level, preflashing of the WFPC CCDs is needed in order to overcome the severe nonlinearity (deferred charge) at low levels of non-uniform illumination with high spatial frequencies. Finally, faint (undersampled) stars in Wide-Field Camera images may not be distinguishable from weak cosmic ray events because both signals will produce significant amounts of charge in only a very few detector elements.

In conclusion, we stress that it is the combination of the characteristics of astronomical targets in the spatial and spectral regimes with the performance of HST that makes the acquisition of an a priori experience so indispensable for the preparation of valuable observations and for their subsequent processing.

3. The Model Package

Conceptually, a realistic simulation of astronomical observations is nothing else but an inversion of the data reduction path. The latter consists of, e.g., resampling from pixel to wavelength domain, deconvolution with instrumental profiles, extinction corrections and calibration with instrumental sensitivities. Instead, the modelling software will start with a clean target (image or energy distribution), will then modulate the signal by including interstellar extinction, redshift, etc. and deterioriate it further by applying all the effects intrinsic to the assumed instrumental set-up. The latter include for example the point spread function, dispersion relation, filter transmission, detector sensitivity, intensity transfer function, scattered light, photon statistics and detector noise. A model package will have to be very modular in order to provide flexibility at the input stage, i.e. the generation of astronomical targets and to remain adaptable to new instruments, configurations and changes of technical data.

It seemed natural to develop the model as a package of application programmes, data bases and command language level procedures embedded in the environment of the large astronomical data analysis system MIDAS produced and maintained at ESO (see Banse et al., *The Messenger,* No. 31, p. 26, 1983). This concept results in several advantages. Firstly, only a very few highly specialized FORTRAN level programmes had to be written from scratch, while all the data handling, display, hardcopy and image arithmetics needed was already covered by MIDAS system commands. Secondly, knowledge of the instrument configurations could be maintained in the model in the form of look-up tables, and the flow chart of the photons through the instruments in the form of command procedures which activate individual system commands. This scheme provides for easy debugging, updating and upgrading. Thirdly, the astronomical data (e.g. extinction tables, sample spectra and images) needed for the target generation are stored in an expanding data base accessible to all MIDAS users. Finally, any addition of application programmes to the general MIDAS system or to the HST Model package will be beneficial for the users of either software environment.

The model is structured into 3 major components, namely TARGET GENERATION, OPTICAL PATH and DETECTION. Targets as seen at the entrance pupil of HST come in three major flavours, i.e. 2 D images, point source

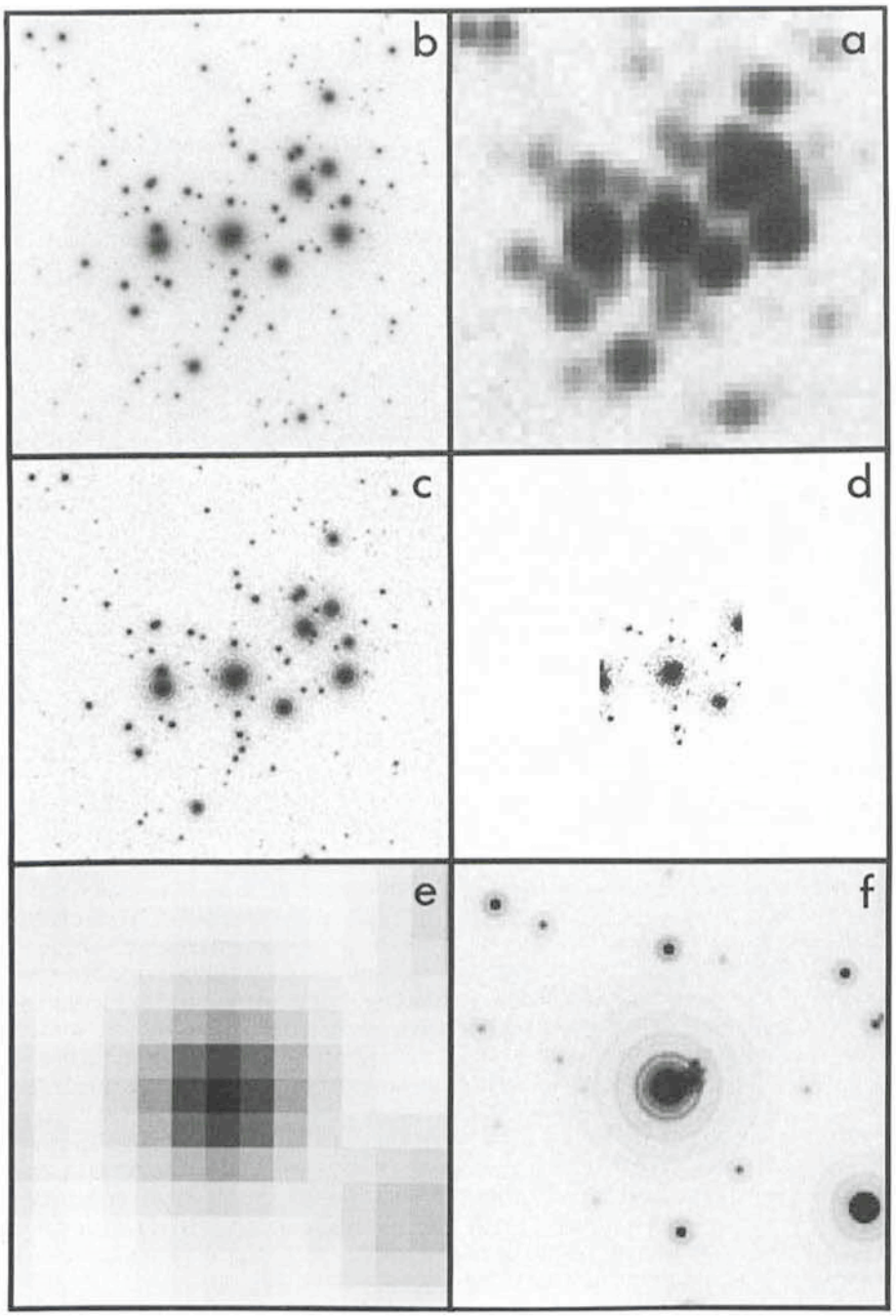

Figure 1: *Simulated images of the Pleiades at 120 kpc distance. (a) ESO 3.6 m, prime focus CCD, seeing 0.5 arcsecond, 3 minutes. (b) FOC f/48 (= PC), (c) FOC f/96 and (d) FOC f/288 — all exposed for 1,000 seconds through B filter, (e) and (f) are enlargements of the central parts of (a) and (d).*

catalogues and energy distributions. In principle, a target will be a multi-dimensional data entity providing monochromatic irradiance as a function of position, wavelength and time. Sampling intervals and size in either of the 3 domains will depend on the particular instrument configuration chosen and the analysis to be performed. For example, targets for imaging will be rather large in the spatial domain but will be sparsely sampled in the wavelength regime, while targets for spectroscopy will eventually carry no spatial information at all but will have a very good resolution in the spectral domain. Target generation includes also various backgrounds, redshifting, reddening and scaling in space and photon flux.

The optical path includes all effects encountered between the HST orbit (e.g., scattered light from sun, moon, and earth, airglow, Doppler shift, aberration) and the detectors (e.g. reflectivities of mirrors, filter transmissions, dispersion relations, geometric distortions, point spread functions). Finally, the actual acquisition of the data (DETECTION) is handled in specific modules that include particle events, intensity transfer functions, quantum effficiencies, read out noise, and the pixel-to-pixel variation of these parameters for the different detectors.

Several data bases are provided with the package. An ASTROPHYSICAL DATA BASE contains extinction tables, spectral catalogues with low and high resolution sample spectra, model atmospheres, images of galaxies, star clusters, H II regions and planetary nebulae, and line lists for emission-line objects. The HST INSTRUMENT DATA BASE comprises for example filter transmissions, detector efficiencies, dispersion relations, intensity transfer functions and flat fields, the HST DATA BASE mirror reflectivities and point spread functions. Astronomical targets and results generated by the users are archived and provide a growing data base for further applications.

In summary, the model package performs the following tasks:

1. Creation and modification of realistic astronomical targets, based on real and/or artificial data.
2. Observation of these targets with different instrumental configurations.
3. Acquisition of data including the peculiarities of the detectors.
4. Use of the general MIDAS environment to modify, hardcopy and analyze the data at any intermediate step.

4. Examples

In the remainder of this article we present some examples obtained with the model package. Rather than discussing all the details of a particular case we emphasize the differences between ground-based experience and expected HST results. More details on the HST PSF and sampling problems can be found in papers by King (1979; *PASP* **95,** 163) and Bendinelli, Di Iorio, Parmeggiani and Zavatti (1985; *AA* **153,** 265), on the appearance of WFPC images of Local Group galaxies in a paper by Hoessel and Danielson (1985; *PASP* **95,** 336).

4.1. The Pleiades at 120 kpc distance

Figure 1 shows artificial images of an open cluster that has been generated using the brightest 300 members of the Pleiades but scaled in position and brightness to a distance of 120 kpc. This distance, in fact about 2 times the LMC distance, has been chosen in order to squeeze the cluster into the field of the FOC f/96 mode. Note that no additional field stars have been added and that a flat background of 25 mag per square arcsec has been assumed. The brightest star mapped has a B magnitude of 17 mag, the faintest ones are at about 29 mag and contribute only statistically to a slightly enhanced

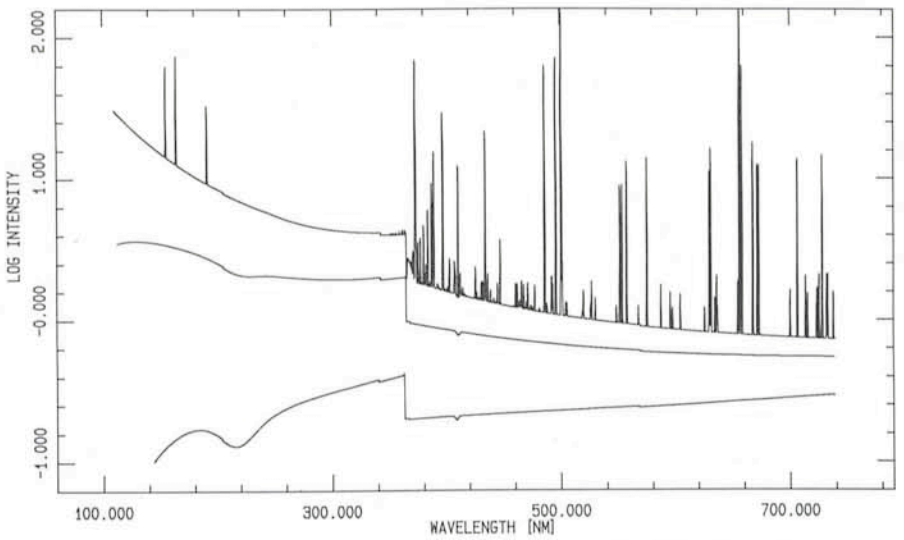

Figure 2: *Simulated spectrum of a planetary nebula. The effect of interstellar extinction on the continuum is shown for an LMC extinction law at E (B–V) = 0.15 and 0.5 mag, respectively.*

background level. Figure 1a shows a 180-second integration on a CCD mounted at the prime focus of a 4-m class telescope. A gaussian seeing profile of 0.5 arcsec FWHM has been assumed. Figures 1b through 1d show Planetary Camera (or FOC f/48), FOC f/96 and FOC f/288 images. Exposure times would have been 1,000 seconds each through B band filters. Figure 1e and 1f zoom in on the image of the brightest star in the centre of the cluster as seen from the ground and in the FOC f/288 mode, respectively. In interpreting "excellent-seeing" ground-based images of mysterious objects, i.e. R 136a in 30 Doradus, one may occasionally wish to compare these two images. They demonstrate how much structure can be hidden behind a 0.5 arcsec seeing profile and a high background level.

Fairly obvious is the increase in resolution but more interesting at this point is the notable undersampling of stellar images in the PC or FOC f/48 frames (even more severe for WF). In the extreme case (WF) a blue PSF of 0.02 arcsec FWHM is sampled with pixels of 0.1 arcsec width, leading to triangular, square, or bar-shaped images of faint stars with only 1 to 4 significant pixels. A pre-requisite for successful application of photometry packages that employ scaling of a PSF to measure magnitudes in crowded stellar fields (eg. DAOPHOT) will be the acquisition of multiple frames slightly shifted by fractions of a pixel size with respect to each other (in order to satisfy the Nyquist theorem in two dimensions). Note also the fringing of bright stars, the exact pattern of which will depend on effective wavelength in broad bandpass filters. Point spread functions of HST and associated problems have also been discussed recently by Bendinelli, Di Iorio, Parmeggiani and Zavatti (1985; *AA* **153,** 265).

Since we used a point symmetric PSF and did not include the diffraction pattern of the spiders, speckle patterns due to misalignments and non-ideal mirror figures, scattering by microroughness and dust on the mirrors, one should consider the images of the brighter stars only as the currently best guess of what an azimuthal average over a stellar image would look like. This is especially true for the FOC f/288 mode. Laboratory simulations of speckle images in the f/288 mode have been presented by Lohmann and Weigelt (ESA/ESO Workshop on "Astronomical Uses of the Space Telescope", F. Macchetto, F. Pacini and M. Tarenghi (eds.), ESO, 1979, p. 353) and Weigelt (ESO Conference on the "Scientific Importance of High Angular Resolution at Infrared and Optical Wavelengths", M.H. Ulrich and K. Kjaer (eds.), ESO, 1981, p. 95) for example.

4.2. FOS spectra of a faint planetary nebula in the LMC

Figure 2 shows the modelled energy distribution of a planetary nebula plus its central star in the LMC, m (B) = 20 mag. We used a 100,000 K black body, the relative emission-line strengths of NGC 7027 and a nebular emission continuum, all ingredients properly scaled for an observation in a 0.5 arcsec aperture. In addition, a weak H(gamma) absorption line has been added as an example of the stellar absorption spectrum. Two continua without nebular emission lines have been drawn for interstellar extinction in the LMC with E (B–V) = 0.015 and = 0.5, respectively. A scientific objective of these simulations would be the evaluation of the best instrumental configurations and the exposure times required for a proper analysis of such objects with the Faint Object Spectrograph.

Figure 3 shows the count-rates obtained for the input spectrum with E (B–V) = 0.15 in the low resolution modes G 160 L plus blue digicon and G 650 L plus red digicon, respectively. The figure also makes the missing spectral coverage of the region between 240 and 380 nm by the FOS in its low resolution mode quite evident. A fully-fledged simulation is presented in Figure 4 where the final "raw observational" data of a 1,000 second integration using grating G 400 H and the blue digicon is shown. Note that at this spectral resolution and with the signal-to-noise ratio (SNR) obtained, the broad absorption underlying the H-gamma emission is invisible.

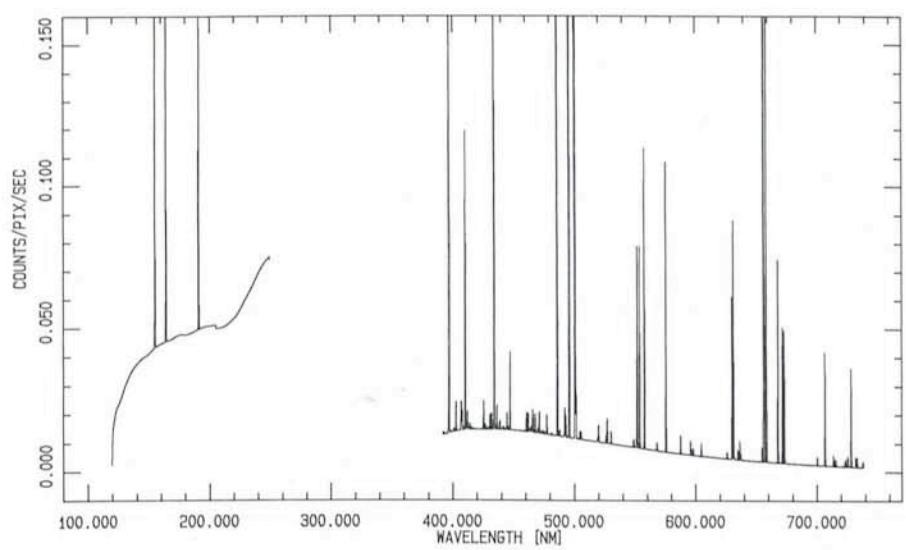

Figure 3: *Count rates in FOS modes G 160 L (blue digicon) and G 650 L (red digicon) using as input the spectrum with E (B–V) = 0.15 mag from Figure 2.*

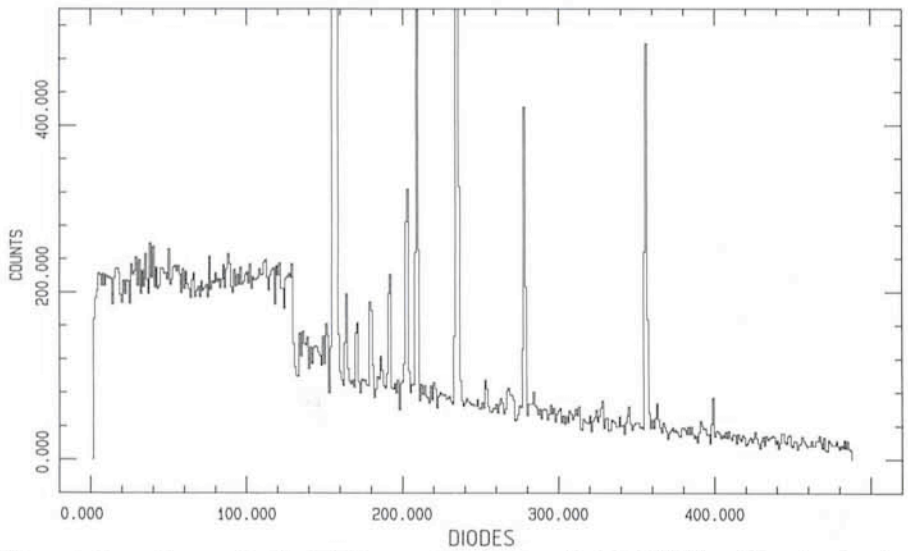

Figure 4: *Raw data acquired in 1,000 seconds in FOS mode G 400 H (blue digicon) using the same input as in Figure 3.*

The simulations demonstrate clearly the variability of the SNR over the free wavelength range. Furthermore, the assumption that the performance for hot stars is increasing with decreasing wavelength is extremely dependent on the amount of extinction that has to be expected towards the object. Finally, it is noteworthy that in the visual wavelength range the faint object spectrograph EFOSC at the 3.6-m telescope of ESO, La Silla, produces a similar SNR for objects of about 19 mag (B) in 3,600 sec. i.e., only 2.6 times more exposure time.

4.3. Close double stars with a large brightness ratio

The last example focusses on a challenging application of the high-resolution imaging offered by HST in combination with the FOC f/288 imaging mode. Taking the theoretical FWHM (in pixels) of stellar images in the f/288 mode given in the manuals at face value, the detection and resolution of stellar pairs with separations of 0.2 arcsec should be no problem at all. However, if the brightness of the stars differs too much, the (noisy) diffraction pattern of the bright component will render the faint one invisible. To reach this conclusion does not really require simulated observations, but the latter might help to optimize the selection of the bandpass in such a way that the faint component will not be burried in a strong diffraction feature. Yet there is still another effect that has to be considered when estimating exposure times. The intensity transfer function (ITF) of the FOC becomes very nonlinear at typical count rates above 0.6 cts/s/pixel, depending on the actual configuration chosen. The ITF then levels off (saturation) and at more extreme rates quickly drops to zero. This happens long before a lethal level of the illumination is reached. Therefore, depending on the amount of background, even a faint star can actually lead to critical count rates. In Figure 5 we demonstrate this effect for a binary with 0.2 arcsec separation and an intensity ratio of 1/1,000. The top panel displays a cut through the image in photon flux units at the detector (FOC f/288, effective wavelength 170 nm, 256 * 256 pixels), the wiggly wings of the bright stars profile stem from the diffraction pattern which is almost unresolved at this wavelength. The lower panel shows from bottom to top 1,000 sec. integrations through various combinations (as labelled) of the medium bandpass F 170 M filter and neutral density filters

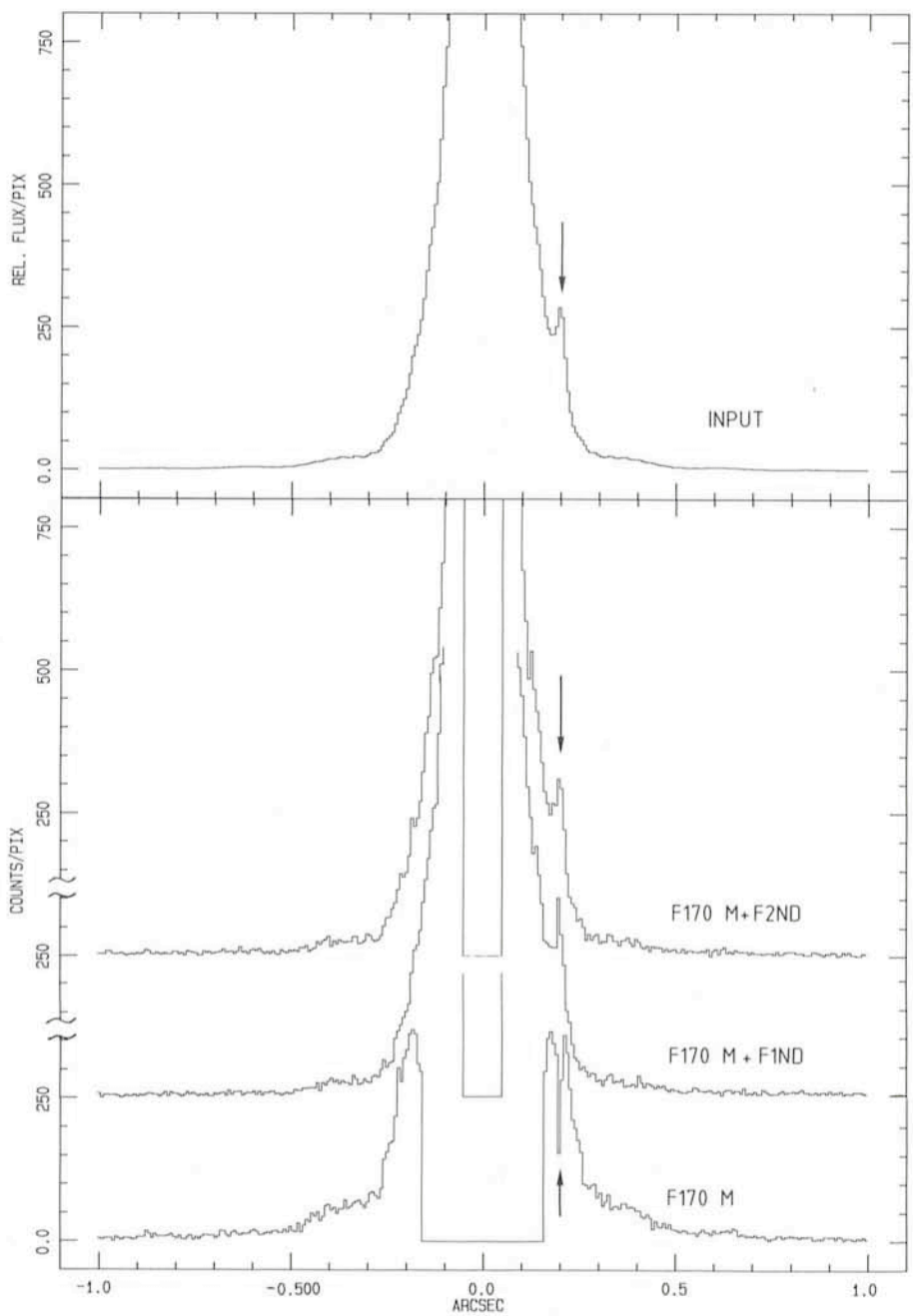

Figure 5: *Slices through FOC f/288 images of a double star with a separation of 0.2 arcsecond and brightness ratio 1/1,000. See section 4.3 for more details.*

of 1 and 2 mag attenuation. Since the example is chosen in such a way that the wings of the bright star are already close to nonlinearity, the SNR in the wings does not change dramatically with the choice of filters. The core of the bright star is therefore always beyond saturation, i.e. at zero level. Note the behaviour of the faint star. Without attenuation it is also subject to oversaturation, i.e., is represented by a hole in the wings of the bright star's image because the faint star's flux is added to this very high background. Adding stronger and stronger attenuating filters actually increases the detectability: With a 2 mag density filter in the beam, the SNR is superior to the 1 mag combination.

This last example demonstrates nicely, how much experience can be gained from mere simulations. Obviously, there will always be observations that reveal the unpredicted and therefore cannot be anticipated during simulations. What can be learned, however, is the awareness of problems that may be unimportant under certain circumstances (which usually are not encountered by most ground-based observing programmes) but can determine completely the outcome of another type of observation.

5. Availability

The model package is available for use at the ST-ECF, ESO, Garching. Online help facilities, a Users Guide and documentation of the Data Bases are provided. Although its main purpose is to simulate HST observations, it can easily be adapted to other instrumentations as well, and we anticipate that the instrumental data of cameras, filters and spectrographs in operation at ESO, La Silla, will become available. Prerequisits for a successful use of the model are experience with the MIDAS system, a detailed prescription of the astronomical target to be generated and familiarity with the HST Instrument Users Guides applicable. A minimum of 3 days should be allocated for a typical project. Prospective users should contact the ST-ECF for details, arrangements of staff support and booking of computer time.

6. Acknowledgements

Besides ST-ECF staff, the following individuals and groups have contributed data, software, and discussions: K. Banse and D. Ponz (ESO Image Processing Group), members of the Instrument Support Branch and others at the STScI, in particular S. Ewald, G. Hartig and F. Paresce. D. Carr and C. Prasch were involved in most of the laborious work of extracting and editing the instrument data base, etc. from handbooks and other sources. Finally, all those collegues who have used the model during its evolutionary phase have contributed valuable comments and complaints.

NEWS ON ESO INSTRUMENTATION

The ESO TV Autoguiders

M. DUCHATEAU and M. ZIEBELL, ESO

In February 1985 four new autoguider systems have been installed at La Silla. The 3.6-m telescope, the CAT, the 2.2-m telescope and the Schmidt got equipped with a system.

They have been used now successfully for one and a half year and we hope that they are not "job killers" but that in the meantime they have been accepted as an improvement of work conditions.

Three main reasons induced us to use low-light-level TV cameras for autoguiding:

1. There were already 5 telescopes at La Silla equipped with TV cameras for manual guiding.
2. An electronic crosshair already existed and by setting several electronic signals for it the development of the autoguider was simplified.
3. Long experience with manual guiding on the Schmidt telescope's electronic crosshair encouraged us to continue in the same direction. The stability of the deflection system of the TV camera did not create any difficulty.

The idea was therefore to use the video signal of a TV camera in connection with an electronic crosshair as shown in Figure 1:

Except for the TV camera, all the components are installed inside the control consoles. In some locations, the digital memory used for scan conversion in case of an integration facility does not exist. The video signal is then connected directly from the TV camera to the autoguider chassis (Fig. 2). The advantage of this solution is that no mechanical and no optical modifications are needed in the focal plane.

Electronic Crosshair

The electronic crosshair, developed to perform corrections for differential refraction on the Schmidt telescope, produces on the monitor one fixed cross, one movable and a rectangular box around the centre of the movable cross-

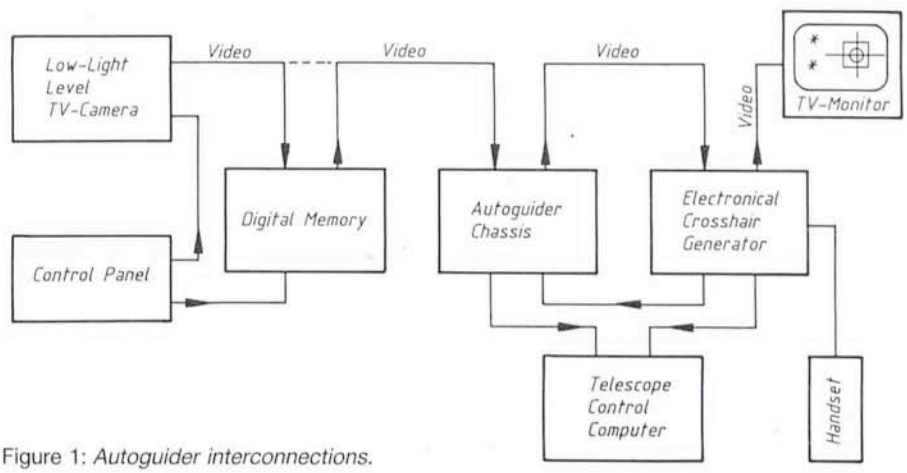

Figure 1: *Autoguider interconnections.*

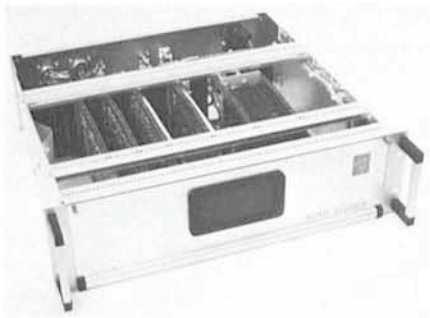

Figure 2: *Autoguider.*

hair accordingly. In manual guide mode the observer has to follow with his guide star the movable crosshair by correcting the telescope position. With special software the movable crosshair can be used (and it is used so on the Schmidt telescope) for comet tracking.

All the delays which are necessary to build up the cross are produced digitally and do not suffer from temperature effects. The size of the box is adjustable by a handset to fit it to the apparent star diameter under different seeing conditions. The movable crosshair and the box create 4 quadrants. The video signal inside each of these quadrants is integrated and the equilibrium between the four fields is used for autoguiding. All the digital signals for the box (beginning, middle and end in horizontal and vertical direction) are provided by the crosshair and connected to the autoguider.

Autoguider

The basic principle of the autoguider is shown in Figure 5.

Corresponding to the 4 quadrants on the monitor created by the electronic box and the movable crosshair, 4 digital integrators are used to integrate the light over the surface of each quadrant and over an adjustable number of frames. The digital integrator is built out of a 32 bit full adder and a 32 bit register. Each of the registers I_1, I_2, I_3 and I_4 is in reality built up out of 2 registers (I and II). Registers I and II contain in principle the same information, register I is just used to produce a short delay before

Figure 3: *Crosshair generator.*

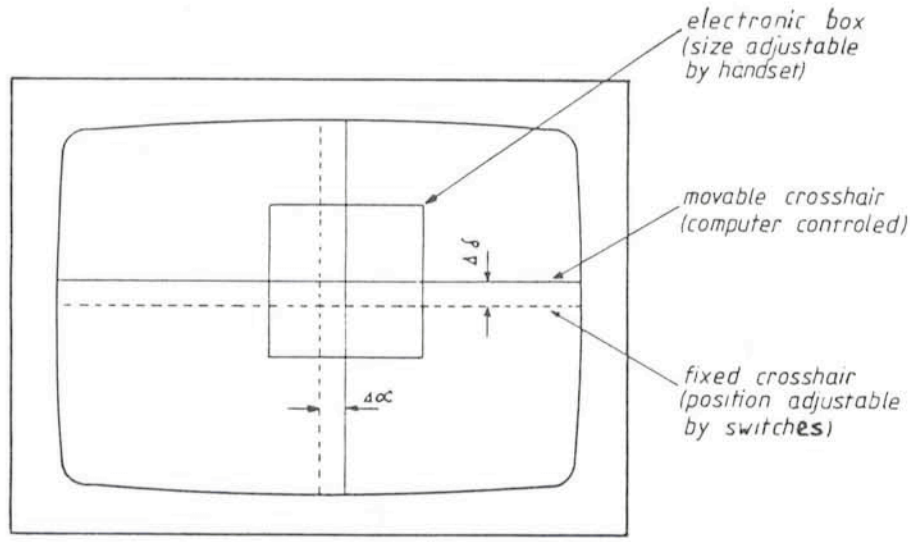

Figure 4.

the information appears at the output of register II. One full adder is commonly used by the 4 channels. After a new conversion of the A/D converter the digital output is transferred via S2 to the full adder and added to the former value which was stored in register II and is now memorized in register I with a certain delay. The new sum is transferred to register II and can be added to the next pixel value. The complete cycle of A/D conversion, integration and transfer to the register takes less than 200 ns. To be more or less independent on different TV cameras, on different black levels (influenced by sky background illumination) and on different dc levels, a special signal clamp has been added in front of the A/D converter. Driven by the switch logic (controller) a Sample & Hold amplifier memorizes the actual analogue voltage of the video signal when the readout beam of the TV-camera passes into the quadrants at the left side. This analogue voltage is then used as a reference for the A/D converter. This method ensures that only the star light inside the 4 quadrants is integrated with no additional DC level. It makes the autoguider very sensitive and allows automatic guiding on very faint objects. At the 2.2-m telescope stars down to 19th magnitude have been used for autoguiding when using the Boller & Chivens spectrograph. Figure 6a illustrates one TV line which passes through the upper left and upper right quadrant in combination with the modulation signals for the electronic crosshair.

A flag appears on the controller board at the end of the integration time, which can be choosen in a number of frames with a thumb wheel switch behind the front panel. The computer is continuously scanning this bit and when it recognizes "end of integration" it reads the

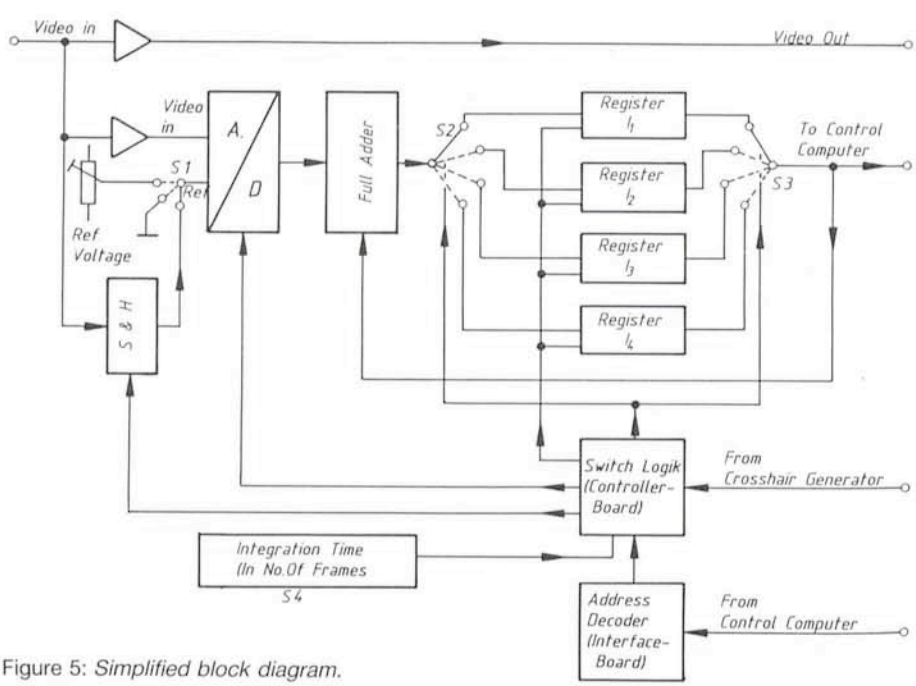

Figure 5: *Simplified block diagram.*

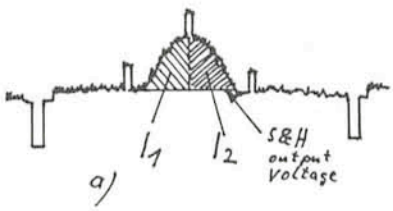

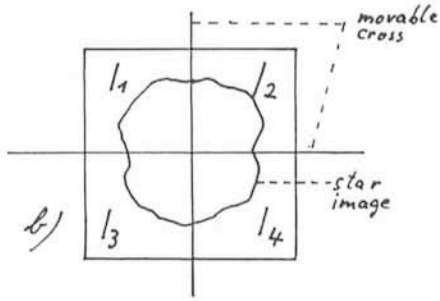

Figure 6a and b.

four integrated values. The address decoding is done on the interface board. When the computer has read the last address all the registers are cleared and a new integration starts automatically.

In the computer the position error is calculated and normalized by:

$$E_x = \frac{I_1+I_3-I_2=I_4}{I_1+I_2+I_3+I_4}$$

$$E_y = \frac{I_1+I_2-I_3-I_4}{I_1+I_2+I_3+I_4}$$

(See Fig. 6b)

The normalization makes the error independent on star magnitudes, seeing effects and HV adjustments of the TV cameras. To keep the servos of the main drive axis of the telescope stable, an additional measure is to avoid an error proportional speed correction. If an error is detected the corrections will be done by constant offset steps in the right direction.

If the normalized error is bigger than 0.15 then an offset step of 0.1 second of arc is applied. If the error is bigger than 0.85 the offset step will be 0.5 second of arc, but this value can be adjusted depending on optical scales and seeing conditions. For an optical scale of 2.5 lines per second of arc the appropriate step size would be 0.″3. If the error is smaller than 0.15 no correction will be applied.

ESO Infrared Specklegraph

C. PERRIER, Observatoire de Lyon, France

Introduction

An infrared specklegraph is available for Visiting Astronomers for use at the 3.6-m telescope F/35 focus. It has briefly been described in the Announcement for Applications in periods 36 to 38. First tested in September 1984, it has since then achieved the expected performances during several runs. However, its theoretical limits have actually been reached only after a dome air-cooling system has been put into operation early this year. In this article we introduce the instrument assuming that the reader already has some knowledge of the short-exposure imaging principles.

The system is based on the slit-scanning technique which allows to obtain one-dimensional images, that is profiles of a source projected onto the scanning direction axis. It aims first of all to diffraction-limited observations; therefore, it is designed for a data rate fast enough to acquire images under conditions of quasi-frozen seeing, and for a spatial sampling adapted to the near-infrared range. The data are stored in the form of individual scans and the data reduction basically yields coadded scans and 1-D visibilities, i.e. Fourier transforms of the source intensity distribution. These visibilities can then be used either directly for size measurements using assumed intensity distribution models or as input to image restoration algorithms.

Instrument Concept

A dedicated dewar equipped with a set of slits and an electronic chain providing a good frequency response is mounted at the F/35 focus on the infrared photometer adaptor (for a description see Moorwood and van Dijsseldonk, *The Messenger,* No. 39, p. 1). The secondary mirror is used to sweep the beam onto the slit and for that purpose is driven with a saw-tooth waveform. During each sweep equally-spaced measures of the flux integrated along the slit are acquired, forming a 1-D image or scan. Rotating the photometer and secondary mirror adaptors gives access to any given position angle (PA).

The requirements have led to an instrument that is a good compromise between good sensitivity in a wide electric bandpass and the specific constraints imposed by the standard infrared instrumental framework. Its current characteristics are shown in Table 1. The system has been optimized for use at L and contains slits adapted to the telescope cut-off frequencies at K, L and M, plus a wide one for medium-resolution imaging. The maximum data rate well matches the less good conditions under which it is still feasible to obtain high-resolution data down to 2 μm: atmospheric correlation time $\geq$ 20 ms and seeing at V $\leq$ 3 arcsec. Conversely, the scan time and amplitude may be continuously adjusted up to values sufficiently large to benefit from excellent conditions occurring when the seeing varies slowly. The full resolution of the 3.6-m telescope cannot be achieved at J and H because the usual observing conditions would be too demanding in terms of frequency response; however, it is of course feasible to observe at these wavelengths with the resolution for K.

Part of the acquisition chain is common to both speckle and photometric set-up; this insures some useful standardization. On the contrary, they do not

TABLE 1: SPECKLEGRAPH CHARACTERISTICS

Filters:	wide-band:	J H K LA M
	CVF:	2.43–4.48 μm; 4.26–5.32 μm; resol. ~1/70
Apertures:	diaphragm ∅:	1.5 4.0 10. arcsec. (saturate at M)
	slit width:	0.105 0.159 0.221 arcsec. (5 arcsec. high)
		0.156 0.246 0.464 arcsec. (10 arcsec. high)
Optics:		F/35; linear beam
Detector:	type:	Cincinnati hybrid InSb; – GΩ feedback
	frequency response:	0.8 @ 100 Hz; 0.4 @ 500 Hz
Electronics:	input range:	± 2.5 V after ± 9 V offset & ×1–1024 amplification
	dynamics:	4096 ADC units
Scanning:	wave-form:	saw-tooth linearity < 1 % in useful part
	amplitude:	0–40 arcsec. (for 128 pts)
Sampling:		128 or 256 pts/scan; half for source; half for sky
		20–600 ms/scan (for 128 pts)
Cryogenics:	outer can:	liquid N2; 6–12 h hold time
	inner can:	solid N2 (55–60 K); > 1–2 weeks hold time

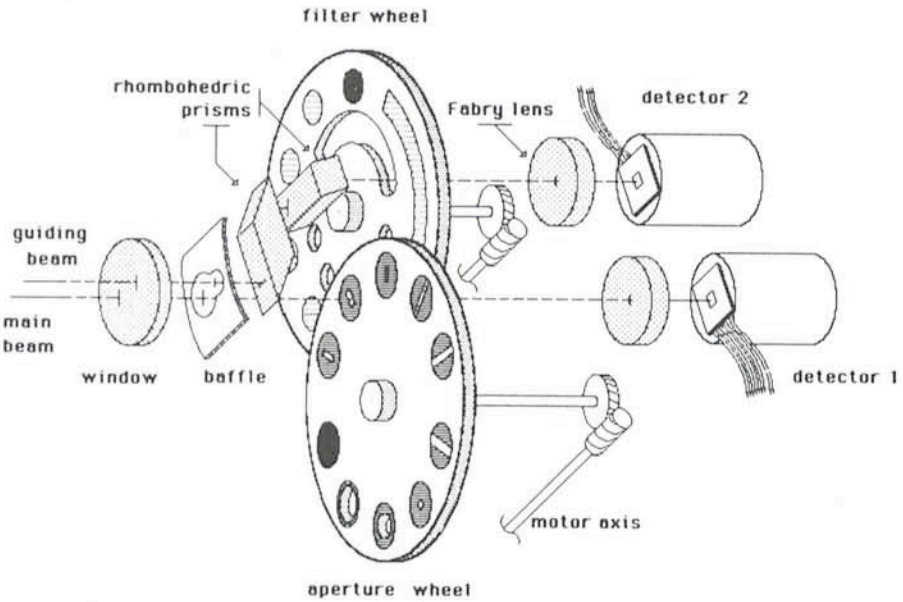

Figure 1: *Schematic of the cold optics.*

share any of the control software nor of the acquisition procedures. In speckle, the secondary mirror control itself is actually part of the acquisition software rather than of the distinct F/35 programme known to infrared observers. The data tape formats also differ largely. So, while the specklegraph might be thought of as a mere additional dewar to be used within the infrared photometric frame, it would not be practicable to change from one set-up to the other during the night.

Optical and Mechanical Design

The cooled optics schematic is given in Figure 1. The very small throughput of the dewar, when used with a slit, has made it possible to choose a linear optical path without pupil reimaging on the filter. This yields a very good beam profile, quite useful for extended sources scanned with a long slit so that very little loss can be expected from this optical arrangement. The use of a Fabry lens has the drawback of chromatism: the optimum adjustment has been done at L which is the best compromise between infrared speckle advantage and degrading sky noise when the wavelength increases.

Figure 1 indeed shows two beams; only the main one is referred to in Table 1. The second one, 8 arcsec off-axis, was initially intended for guiding and seeing monitoring and is equipped with a Santa Babara InSb mounted with a 1 GΩ feedback, a 0.8×5 arcsec^2 slit and an L filter. But the second digitization chain is currently not implemented. Although it can in principle still serve in an analogic way for guiding, practice has proven that this is of little interest as the main beam itself does it more conveniently until the limiting magnitude, depending on seeing conditions, is reached. In fact, this turns out to be more accurate, in the scan direction, than using a guide-star acquired off-axis with the infrared adaptor TV acquisition system. Guiding remains a manual task as scanning prevents the use of the auto-guiding system.

It must be realized that the slits have a fixed orientation (horizontal for a vertical dewar position) whatever the scanning direction on the sky is. As scanning must obviously be perpendicular to them, both adaptors (Cassegrain and secondary mirror) have to be rotated at each new PA setting. While this is straightforward for the latter, it is more time-consuming and requires much caution for the former. The change of PA is thus better restricted to a minimum during the night.

Operation

All instrument functions, that is those of the specklegraph and of the secondary mirror adaptor, are remote-controlled from the User consoles much as in photometry. The software also includes on-line data reduction facilities yielding individual or averaged scans, averaged power spectra and preliminary visibilities and follows the ESO interfacing rules with commands entered either by typing or function keys. The status of the instrument is displayed and updated during acquisition. The DC signal from the detector appears on an oscilloscope which displays every instantaneous image; this is of great help for adjusting the offset and amplification parameters,

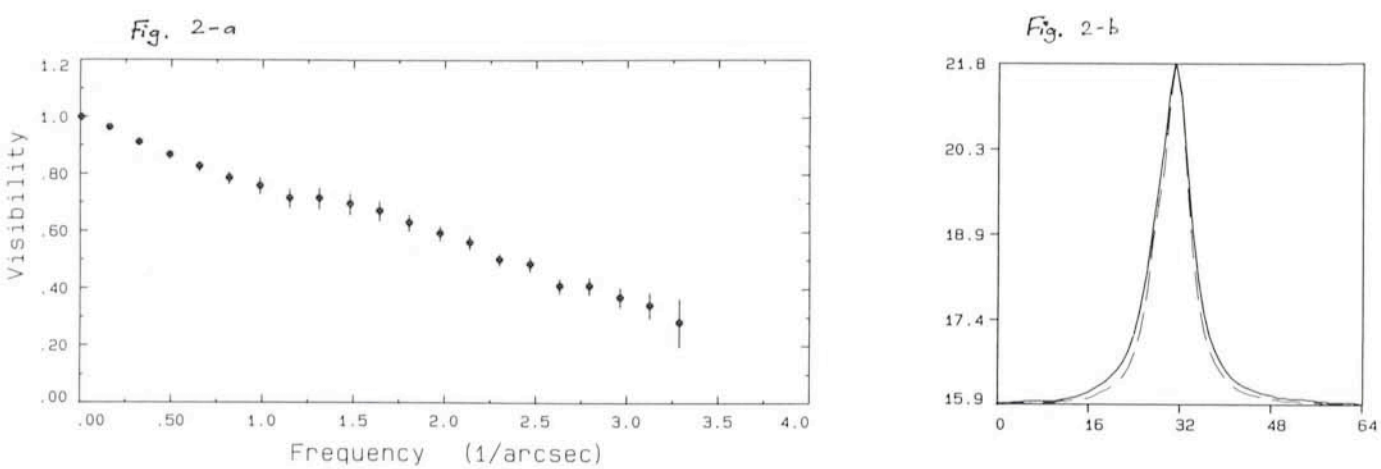

Figure 2: *(a) Visibility at L of an "extended" source. Magnitude at L: 3.5. Exposure time per scan: 100 ms. 1,600 scans retained out of a 16-mn total observing time (reference included). A fit with a 2 gaussian components model gives a diameter of 0.18 ± 0.01 arcsec for the core, contributing 84 ± 3% of the total flux, and 1.5 ± 0.3 arcsec for the halo.*
(b) Coadded recentred scans from the same set of data as in (a). Seeing at V: 1.6 arcsec; full scale: 6.0 arcsec. The dashed curve results from the same treatment applied to the reference star. This graph illustrates the potential access to true imaging by deconvolution techniques using these profiles.

TABLE 2: SPECKLEGRAPH PERFORMANCE

Band:	K	L	M	CVF (3.6 μm)	CVF (4.6 μm)
Limitation source:	system	backgr.	backgr.	system	backgr.
Maxi. spatial frequency (*):	7.9	4.8	3.7	≈4.8	≈3.7
Rayleigh resolution (''):	0.13	0.21	0.27	≈0.21	≈0.27
Saturation with diaphragm:	0.2	−0.4	−1.7	−3.6	−4.2
HIGH RESOLUTION (*)					
Limiting magnitudes m_o:	7.7	7.0	5.8	4.6	4.5
MEDIUM RESOLUTION (•)					
Limiting magnitudes m_o:	13.6	11.3	9.3	8.9	8.1

(*) in arcsec^{-1}.
('') in arcsec; it gives the size of a source which would be completely resolved; practical resolutions may be 2 or 3 times better depending on the S/N.
(*) Visibility S/N at half resolution: 10, T_t: 15 mn, T_e: 100 ms, W: 1.0 arcsec, s ≈ $1/f_c$. S/B ≈ $W^x T_e^y T_t^y s^z$ with x = −4, y = 1/2, z = 2 (sys. lim.), 1 (back. lim.).
(•) Averaged image S/N per seeing element: 3, T_t: 15 mn, T_e: 500 ms, W: 1.0 arcsec, s: 0.46 arcsec, x = −1/2, y = 1/2, z = 1/2 (sys. lim.), 0 (back. lim.).

monitoring the background level and, as mentioned before, fine guiding, but also provides a quick estimation of the atmospheric correlation time t.

Two principles guide the observing procedure: each scan on the source is followed by a scan of equal length on the sky for later sky noise compensation (the scan is thus more than twice the quoted exposure amplitude) and any set of scans on the programme source must be connected to another set on a point-like star (the reference) – obviously with strictly identical settings – in order to correct for the mean atmospheric and optical transfer functions.

One must distinguish between three stages in the course of the observations: the amplitude calibration, usually done once a night on double stars with accurate astrometry (there are not so many); the frequent instrumental parameters setting, specific to each source and including focusing and exposure time adjustement to t.; the acquisition itself, one measurement typically lasting 15 to 30 minutes. Two acquisition modes are available: a static mode where the programme object and its reference star are observed separately, that is by two sequential measurements; a source-switching mode which alternates both sources several times within a unique measurement by offsetting the telescope automatically. This latter procedure, with a switch every 2 to 3 minutes quite specific to speckle interferometry, must always be preferred, the former one being restricted to calibrations or special needs. Because it involves so many parameter settings, it usually seems rather complicated to initiate; however, this is the *only way* to override the seeing variations which decide on the final signal-to-noise ratio, at least for not too faint sources. Its efficiency is optimum for close pairs (< 1°) where the differential pointing, performing extremely well (recentring within half an arcsec happens to be unnecessary after switching!), provides a large gain in total observing time over the static mode in addition to an invaluable qualitative gain. The separation of 1° has been found to be the practical limit beyond which differential seeing effects and optical transfer function variations may not be corrected for.

The basic observing procedure just described does not rule out the need to optimize the operation setting for specified purposes; these go from maximum resolution scanning, which requires a standard speckle setting with fast scans and a slit adapted to the telescope cut-off, to medium resolution imaging and/or close stars photometry, which is better done with slow scans, large amplitude and large slits. These two examples are grossly related, respectively, to the study of very compact sources of magnitudes well below the limiting ones and of somewhat extended, possibly multiple, sources of magnitudes reaching the limits. The software is designed for a large range of parameters and permits such opposite settings, but this flexibility will also not prevent a wrong choice like too long an exposure time under fast seeing or too wide a slit for the desired resolution!

Performances

High spatial resolution imaging is extremely dependent on the seeing quality. It can be shown that optimizing according to the atmospheric conditions leads to a S/N dependence on the seeing angle W of the form S/N ≈ $W^{-4 \text{ to } 5}$ The total integration time and the exposure time have a much smaller effect (see Table 2). This means that the source magnitude and the seeing alone almost completely drive the quality of the result or, conversely, that it is *unrealistic* to intend to compensate for poor observing conditions by much longer integration times. On the contrary, the accessible resolution must be derived from these conditions and the

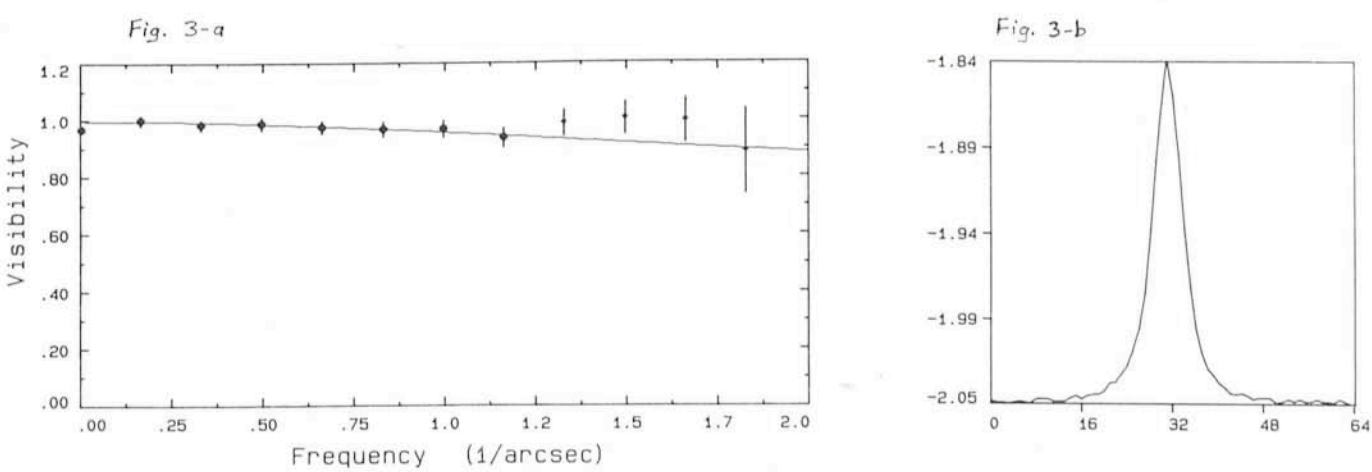

Figure 3: *(a) Visibility at K of a source of magnitude 8.9 observed with the 0.46 arcsec wide slit. Exposure time: 250 ms. 2,700 scans retained out of a 96-mn total observing time (reference included). The solid line is a binary model fit with a secondary fractional flux ratio of 6.5 % drawn for deriving the maximum separation consistent with these assumptions and data (0.20 arcsec).*
(b) Coadded recentred scans from the same set of data s in (a). Seeing at V: 1.3 arcsec; full scale: 6.0 arcsec. A source of a K magnitude 14.5 would be 3 times higher than the rms noise and would clearly show up if it were at more than 1 arcsec from the central source.

relevant parameters (slit width, exposure time, amplitude, temporal frequency range . . .) choosen accordingly and modified as those ones change. Here is certainly the difficult side of this technique!

Medium resolution imaging is much less affected by the seeing. The performances are derived by taking into account the system or sky limitations as in photometry. It can be seen (Table 2) that the sensitivity is of course lower than with a photometer but a resolution of 0.5 arcsec can here be routinely achieved. This mode can also be an excellent back-up in case of bad conditions.

Examples showing the result of two opposite optimizations are shown in Figure 2 and 3. The data were obtained under good conditions, yet for Figure 2 the number of scans was not large enough to reach the background limitation. In this case the uncertainty computed at each spatial frequency results essentially from the seeing statistics (note that the values in Table 2 assume a stationary seeing); as contiguous points are not independent, the visibility may present some oscillations which are not real. That is why such a visibility must be fitted by a model of at most 3 or 4 parameters.

Treatment

Some reduction is done in real time aiming to the estimation of the observation quality but the final results rely on a more sophisticated treatment applying algorithms of image selection according to the seeing. Figures 2 and 3 display data from March 1986 reduced in this way with the software available at ESO (at La Silla and Garching, on an HP computer) and show the standard outputs of it. For many sources, these will be sufficient to extract the useful information by means of simple fits. The reduction package includes a fitting module with a model of one to three components of variable size, fractional flux and location; their individual intensity distribution being choosen from a set of analytical functions or stored in the form of a discrete set of intensities.

More elaborate processes like co-added-images deconvolution or image restoration are not currently included in this package. The observer willing to apply his own method can either use the raw data stored on tape as blocs of scans or the files created by the reduction software containing processed data like sorted scans or calibrated power spectra.

Contributions

This specklegraph was designed and integrated under ESO contract at Observatoire de Lyon (sup. F. Sibille), INAG (M. Jegou) and Laboratoire IR de Meudon. The ESO infrared group contributed to the qualification and tests. The software was provided by C. Perrier with support from F. Gutierrez. Special thanks are due to T. Bohl, C. Marlot and J. Roucher who were deeply involved at the integration or testing stages.

The Fast-Photometry Facilities at La Silla

P. BOUCHET and F. GUTIERREZ, ESO, La Silla

We briefly present in this note the available programme (and its environment) to perform fast photometry at La Silla. This facility has become available on the mountain a long time ago already but recent discussions with some Visiting Astronomers tend to show that potential users are not yet well aware of it. Many programmes have already been carried out with this mode of observing, mainly in the infrared but also in the visible. Let us mention, for instance:

– Occultations of stars by planets to discover and/or study rings as well as to determinate the temperatures and variations of the atmospheres of the planets. (See for instance: Bouchet et al., *The Messenger* No. 26, Dec. 1981 and Haefner et al., *The Messenger* No. 42, Dec. 1985).

– The mutual phenomena of Jupiter, observed through the international PHEMU 85 campaign (Arlot et al., same issue of *The Messenger*).

– Search for flare or rapid variations in cataclysmic variables (Motch et al., *The Messenger* No. 26, Dec. 1981).

The "Time Series Photometry Programme" (TSPP) consists of a set of counters that are read each millisecond and can be used at any telescope equipped with a standard 21 MX computer extender, which are presently the ESO 3.6 m and 1.0 m, and the Danish 1.5 m. However, for special cases it could be possible to implement it at the ESO 50 cm too. Up to 4 counters are synchronized with a 1 Kilo-Hertz signal from a CERME clock display unit. This clock is connected to the ESO Universal Time. The computer is connected to the CERME to read out the UT. Every 10 seconds the synchronization of the computer internal time and the CERME time is checked. In case of a lost synchronization, the programme will reset it at the next 10th second change (in that case, 10 seconds of observations would have been lost). The CERME clock provides also a 1 kHz signal to read the counters each millisecond.

The user chooses the time resolution called TBASE. The acquisition is made by adding the counts read each millisecond from the scalers during the time TBASE and saving the sum in a floating point internal buffer. When this buffer is full, it is sent to the magtape unit. This procedure is made through two independent buffers. While one is saving data, the other one is dumping its data to the magtape, and reverse. In this way no data are lost during the external dump.

The computer is also connected to a Strip Chart recorder which enables the observer to see ON LINE the input data at a time resolution selected by him. The programme foresees the possibility to be connected to the ESO Standard photometers to provide control over the filters and diaphragm wheels and over the shutters.

Data obtained from the TSPP acquisition environment can be reduced at the HP-1000 system at the computer centre at La Silla. This is done using several programmes written by Ch. Motch which:

– list a catalogue of all the records present in a magtape file;

– read several consecutive records, plot any part of the data in memory, make a listing of the measurements, change them eventually, compute averages and dump data in a disk file;

– copy records in any file from magtape;

– perform a Fourrier transformation on a block of 2,048 measurements in the same channel;

– compute autocorrelation function on blocks of 2,048 measurements in the same channel.

MIDAS Memo

ESO Image Processing Group

1. New Computer Facilities

The ESO scientific computer facilities were moved into new rooms in the extension of the ESO Headquarters in Garching. The machines in the old computer room were disconnected and moved to the new location in the basement of the new wing on July 16. Since there is no large elevator down to the room, all big items like computer racks, disk drives and tape units had to be taken out of the building and lowered down by a crane as seen in Figure 1. The new computer room contains now most of the scientific computer equipment in ESO including the two VAX 8600 computers, the IHAP HP system, the database machine IDM 500, and the peripherals like disk drives, terminal multiplexer and DICOMED image recording unit (see Figure 2). The ESO archive will also be placed in this room which is fully air-conditioned and fire protected by a halon system. The magnetic tape drives are located in an adjacent room with general access. The user room is now also located in the new wing on the entrance level. All IHAP and MIDAS image processing workstations are placed there in additon to a number of public available terminals connected to the VAX's. Figure 3 shows the half of the user room which is dedicated to MIDAS stations. Furthermore, the main printing and plotting facilities are in a central section of the user room.

Figure 1: *Computer equipment lowered down to the new computer room.*

Figure 2: *The new computer room.*

The Image Processing Group has also moved to new offices just above the user room.

2. Networks

Beside the existing connections through modem and package switching network, ESO will become accessible through the Space Physics Analysis Network (SPAN) and European Academic and Research Network (EARN) during this fall. The connection to SPAN which is based on DECnet has made it necessary to change the node names of the ESO computers. The full new names are ESOMC0 (previously MIDAS) and ESOMC1 (previously LEO) while the short form MC0 and MC1 can be used internally in most cases. For the non-DEC community, an EARN node is being established through a computer link to the MPI computer centre. This will also enable people with access to other networks like BITNET to contact us via their gateway to EARN.

3. Data Analysis Workshop

During the previous ST-ECF Data Analysis workshop in February, there was felt a need for having an extensive discussion on MIDAS issues. To accommodate this wish, it was decided to devote a full day for MIDAS related matters. The first MIDAS workshop will be October 23, 1986, for convenience just after the next Data analysis workshop. This will contain sessions on the MIDAS manual, user feedback, and new applications in addition to the presentation of the design proposed for the portable MIDAS. The programme will be sent out together with other material for the Data Analysis workshop. People interested in participating in the MIDAS workshop should contact either the IPG or ST-ECF.

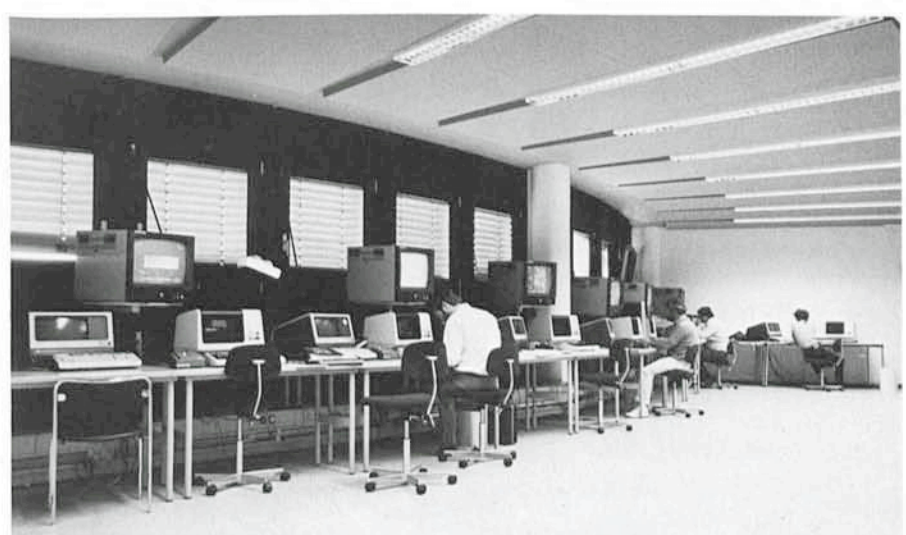

Figure 3: *MIDAS workstations in the new user room.*

Extensions of ESO Headquarters Building Ready

The extensions of the ESO Headquarters building in Garching are now ready. The pictures below show the north-east wing and the new conference room which is housed on its ground-floor. (See also "MIDAS Memo" on page 33 of this issue). The photographs on the opposite page show the extension of the south-west side and the workshop which has been moved into this part.

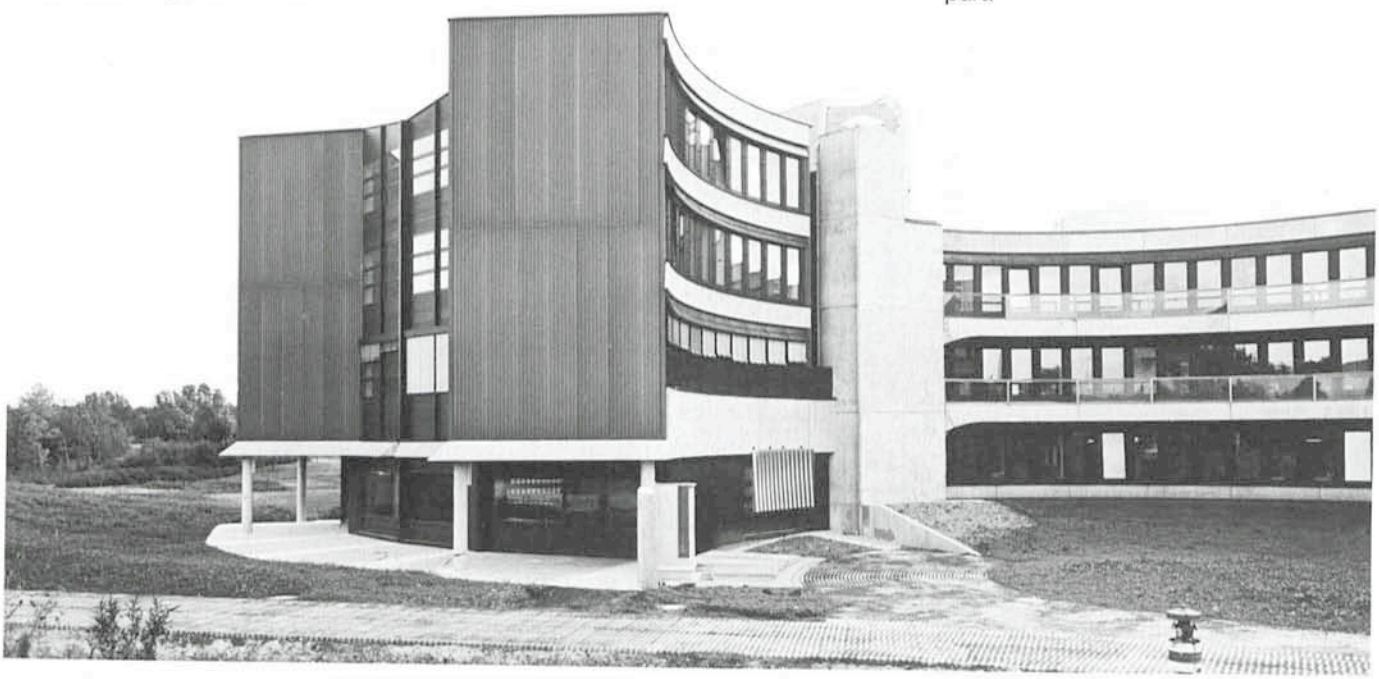

STAFF MOVEMENTS

Arrivals

Europe:

DE ROOS, Rinze (NL), Computer Operator
MARCHAND, Jocelyne (F), Programmer
MEYLAN, Georges (CH), Fellow
MONETI, Andrea (I), Fellow
ROMBOUT, Francky (B), Accounts Clerk

Chile:

DUGUET, Bernard (F), Administrator
HAGSTRÖM, Magne (S), Associate (Microwave Engineer) SEST
JANSSON, Borgar (S), Electronic Maintenance Engineer
WEILENMANN, Ueli (CH), Infrared Instrumentation Engineer

Departures

Europe:

STORTENBEEK, Eduard (NL), Buyer
BAUER, Ruthild (D), Administrative Clerk
JENSEN, Bjarne (DK), Electronics Engineer

Finalizadas las ampliaciones del edificio central de la ESO

Han llegado a su término las ampliaciones efectuadas en el edificio de la ESO en Garching. Las fotografías en la página 34 muestran el ala noreste y la nueva sala de conferencias ubicada en el primer piso.

Las fotografías arriba muestran las ampliaciones del lado sudoeste y el taller que fue trasladado a esta parte del edificio.

ESO, the European Southern Observatory, was created in 1962 to . . . establish and operate an astronomical observatory in the southern hemisphere, equipped with powerful instruments, with the aim of furthering and organizing collaboration in astronomy . . . It is supported by eight countries: Belgium, Denmark, France, the Federal Republic of Germany, Italy, the Netherlands, Sweden and Switzerland. It operates the La Silla observatory in the Atacama desert, 600 km north of Santiago de Chile, at 2,400 m altitude, where thirteen telescopes with apertures up to 3.6 m are presently in operation. A 3.5-m New Technology Telescope (NTT) is being constructed and also a 15-m radio telescope (SEST). A giant telescope (VLT = Very Large Telescope), consisting of four 8-m telescopes (equivalent aperture = 16 m) is being planned for the 1990's. Six hundred scientists make proposals each year for the use of the telescopes at La Silla. The ESO Headquarters are located in Garching, near Munich, FRG. It is the scientific-technical and administrative centre of ESO, where technical development programmes are carried out to provide the La Silla observatory with the newest instruments. There are also extensive facilities which enable the scientists to analyze their data. In Europe ESO employs about 150 international Staff members, Fellows and Associates; at La Silla about 40 and, in addition, 150 local Staff members.

The ESO MESSENGER is published four times a year: normally in March, June, September and December. ESO also publishes Conference Proceedings, Preprints, Technical Notes and other material connected to its activities. Press Releases inform the media about particular events. For further information, contact the ESO Information and Photographic Service at the following address:

EUROPEAN
SOUTHERN OBSERVATORY
Karl-Schwarzschild-Str. 2
D-8046 Garching bei München
Fed. Rep. of Germany
Tel. (089) 32006-0
Telex 5-28282-0 eo d
Telefax: (089) 3202362

The ESO Messenger:
Editor: Richard M. West
Technical editor: Kurt Kjär

Printed by Universitätsdruckerei
Dr. C. Wolf & Sohn
Heidemannstraße 166
8000 München 45
Fed. Rep. of Germany

ISSN 0722-6691

La tarea del Comité de Programas de Observación de ESO

M. C. E. HUBER, Institut für Astronomie, ETH Zürich, Presidente del OPC
J. BREYSACHER, ESO

Los astrónomos de ESO dedican una considerable parte de su tiempo a la preparación de solicitudes para tiempo de observación en La Silla. Sin embargo, debido a la gran demanda por los telescopios, se debe hacer una selección, a veces drástica, de los programas de observación presentados. El Comité de Programas de Observación (OPC) tiene como tarea evaluar el mérito científico de las solicitudes presentadas. Basada en las recomendaciones del OPC, ESO prepara una Lista de Tiempos de Observación en la cual distribuye el tiempo disponible en los telescopios a los programas mejor evaluados.

El OPC consiste de un miembro y un miembro suplente de cada uno de los ocho países que forman la ESO. Junto con un miembro de la ESO, los ocho miembros del OPC revisan aproximadamente 300 a 350 solicitudes que se reciben regularmente en cada período de observación de seis meses. Cada solicitud es evaluada por tres miembros, lo que trae consigo que cada uno de ellos debe leer más de 100 solicitudes dos veces por año. Deben dar una calificación a cada programa presentado y recomendar la cantidad de noches, que a su juicio, debieran de ponerse a disposición del solicitante, siempre que el programa reciba tiempo.

El OPC se reune durante dos días, dos veces por año (una vez por cada período de observación). En estas reuniones gran parte del tiempo se dedica a aclarar las discrepancias de opiniones que existen sobre las solicitudes. Tanto el Director General como el Jefe de la Sección Astrónomos Visitantes participan en estas deliberaciones.

Inmediatamente terminado el OPC, la ESO procede a incluir en la Lista de Tiempos de Observación todas aquellas solicitudes mejor calificadas. Esta es una tarea compleja; muchas solicitudes de observación requieren el uso de más de un telescopio e instrumentación, y otras solicitudes deben adherirse a fechas fijas. Por ejemplo, muchas investigaciones de multi-frecuencia requieren simultáneamente otras observaciones terrestres o en el espacio. Y además existen oportunidades únicas, como por ejemplo ocultaciones estelares por planetas o por la luna, que solo pueden ser observadas durante una noche determinada.

La lista final de Tiempos de Observación es aprobada por el Director General, y aproximadamente dos semanas después de la reunión del OPC se envían los resultados a los solicitantes.

Sin duda el OPC tiene una gran responsabilidad hacia la comunidad, y es por ésto que la tarea de los miembros del OPC es desafiante e interesante. El actual volumen de trabajo para los miembros del OPC se acerca al límite aceptable: si se incluyen las reuniones que duran dos días, y ésto dos veces por año, el tiempo total que un miembro debe dedicar al trabajo del OPC alcanza fácilmente tres semanas e incluso llega a un mes completo por año.

La meta del OPC será siempre de mantener un excelente nivel en los programas de observación. Pero el éxito del OPC se manifiesta tan sólo en la investigación sana, eficaz y fructuosa en toda la comunidad de ESO.

Contents